Elisa Kallioniemi

Electroencephalography responses evoked by transcranial magnetic stimulation on the primary visual cortex

School of Electrical Engineering

Thesis submitted for examination for the degree of Master of Science in Technology.

Espoo 15.8.2012

Thesis supervisor:

Prof. Raimo Sepponen

Thesis instructor:

Ph.D Juha Silvanto

Aalto University
School of Electrical
Engineering

AALTO UNIVERSITY
SCHOOL OF ELECTRICAL ENGINEERING

ABSTRACT OF THE
MASTER'S THESIS

Author: Elisa Kallioniemi

Title: Electroencephalography responses evoked by transcranial magnetic stimulation on the primary visual cortex

Date: 15.8.2012 Language: English Number of pages:8+73

Department of Electronics

Professorship: Applied electronics Code: S-66

Supervisor: Prof. Raimo Sepponen

Instructor: Ph.D Juha Silvanto

By combining transcranial magnetic stimulation (TMS) and electroencephalography (EEG) cortical excitability and connectivity can be studied non-invasively. However, the method is still at an early stage as TMS causes large muscle artefacts to the EEG that are difficult to remove with the existing signal processing methods.

In this master's thesis the combination of simultaneous TMS and EEG (TMS-EEG) was applied to the primary visual cortex. The aim was to use independent component analysis (ICA) to clean the data from artefacts and to explore the neural EEG responses and artificial visual percepts, phosphenes, evoked by the stimulation. The thesis covered a TMS-EEG and a TMS study, which both had five different paired-pulse protocols, a single pulse protocol, and a control protocol. This was the first time ICA was applied to the primary visual cortex EEG, as well as the first time the human primary visual cortex neural responses to paired-pulse TMS were studied.

It was found that ICA removed the TMS-evoked artefacts from the primary visual cortex EEG. In addition, the responses to the paired-pulse stimulation showed no significant differences when compared with the single pulse protocol. Only the spatial spreading of the responses differed significantly. However, the data analysis revealed several problems in the experimental design that need to be fixed before reliable conclusions can be drawn.

Keywords: Transcranial magnetic stimulation (TMS), electroencephalography (EEG), evoked potential, visual cortex, phosphene

AALTO-YLIOPISTO
SÄHKÖTEKNIIKAN KORKEAKOULU

DIPLOMITYÖN
TIIVISTELMÄ

Tekijä: Elisa Kallioniemi

Työn nimi: Primääriselle näköaivokuorelle kohdistetun transkraniaalisen magneettistimulaation aiheuttamat vasteet aivosähkökäyrässä

Päivämäärä: 15.8.2012 Kieli: Englanti Sivumäärä:8+73

Elektroniikan laitos

Professuuri: Sovellettu elektroniikka Koodi: S-66

Valvoja: Prof. Raimo Sepponen

Ohjaaja: Ph.D Juha Silvanto

Yhdistämällä transkraniaalinen magneettistimulaatio (TMS) ja aivosähkökäyrä (EEG) voidaan aivokuoren reaktiivisuutta ja konnektivisuutta tutkia ei-invasiivisesti. Menetelmä on vielä melko vähän sovellettu, sillä TMS aiheuttaa EEG:hen suuria artefaktoja, joita on vaikea poistaa nykyisillä signaalinkäsittelymenetelmillä.

Tässä diplomityössä EEG:n mittaus ja primäärisen näköaivokuoren TMS-stimulointi (TMS-EEG) suoritettiin samanaikaisesti. Tavoitteena oli käyttää riippumattomien komponenttien analyysiä (ICA) artefaktojen poistoon ja tarkastella stimulaation aiheuttamia EEG-vasteita ja keinotekoisia näköhavaintoja eli fosfiineja. Diplomityö käsitti TMS-EEG- ja TMS-mittaukset, joissa molemmissa käytettiin viittä eri paripulssi-, yhtä yksittäispulssi- sekä yhtä kontrolliprotokollaa. Työssä ICA:ta sovellettiin primääriseltä näköaivokuorelta mitattuun EEG:hen ja tutkittiin paripulssiprotokollien aiheuttamia primäärisen näköaivokuoren vasteita ihmisillä ensimmäistä kertaa.

Työssä havaittiin, että ICA soveltui artefaktojen poistoon primäärisen näköaivokuoren EEG:stä. Lisäksi paripulssiprotokollien aiheuttamista vasteista ei löydetty eroavaisuuksia verrattaessa niitä yksittäispulssiprotokollan vasteisiin. Vain vasteiden spatiaalinen leviäminen erosi merkittävästi. Data-analyysi paljasti kuitenkin mittausasetelmassa lukuisia ongelmia, jotka tulisi korjata ennen kuin luotettavia johtopäätöksiä voidaan tehdä.

Avainsanat: Transkraniaalinen magneettistimulaatio (TMS), aivosähkökäyrä (EEG), herätepotentiaali, näköaivokuori, fosfiini

Preface

This master's thesis was written at the Brain Research Unit of the O.V. Lounasmaa laboratory at the Aalto university School of Science during the spring and the summer of 2012. The experimental work was conducted at BioMag laboratory in the Helsinki University Central Hospital.

I would like to thank my instructor Juha Silvanto for giving me the experimental setup and for providing the funding for the study. I thank Pantelis Lioumis for showing me the tricks on how to conduct the TMS-EEG measurements, and for Elyana Saad for helping me with the measurements and all the laughs during the long measurement days. I would also like to thank all my subjects for enabling the study. In addition, during this thesis I was fortunate to discuss with Julio César Hernández Pavón about the TMS-evoked artefacts and ICA, which helped me with the analysis. I am very thankful for receiving this opportunity.

Special thanks for my supervising Professor Raimo Sepponen for great instructions and encouragement. He did not hesitate in offering me enlightening conversations, also about the visual system, even though as engineers it was a mystery to both of us. It was nice to know that whatever problems I had I could always come to ask from you and we could ponder the problems together.

Thanks also to my friend Saila, who guided me with statistical analyses and helped me to choose the proper ones to use, and to Kaisu, who introduced me to TMS some years ago and who patiently supported me through the ups and downs during this thesis. In addition, I would like to thank my family and Iia, the sweetest dog in the world, who made sure that my life was full of happiness during this thesis.

Last but not least, I would like to thank Jukka for endless support and love, and for being there every time I needed you.

Otaniemi, 15.8.2012

Elisa Kallioniemi

Contents

Symbols and abbreviations

Symbols

$\mathbf{B}$	magnetic flux density
$\mathbf{E}$	electric field
T	tesla, the unit of magnetic flux
μ_0	the vacuum permeability
Ω	Ohm, the unit of electrical resistance

Abbreviations

ANOVA	analysis of variance
CS	conditioning stimulus
DBS	deep brain stimulation
DTI	diffusion tensor imaging
EEG	electroencephalography
EMG	electromyography
EOG	electrooculography
fMRI	functional magnetic resonance imaging
ICA	independent component analysis
ICF	intra-cortical facilitation
ICI	intra-cortical inhibition
ISI	interstimulus interval
ITI	intertrial interval
LGN	lateral geniculate nucleus
MEP	motor evoked potential
MOBS	modified binary search paradigm
MRI	magnetic resonance imaging
NIRS	near-infrared spectroscopy
PET	positron emission tomography
rTMS	repetitive transcanial magnetic stimulation
SPECT	single-photon emission computed tomography
tDCS	transcranial direct current stimulation
TMS	transcranial magnetic stimulation
TMS-EEG	transcranial magnetic stimulation combined with electroencephalography
TS	test stimulus

1 Introduction

Transcranial magnetic stimulation (TMS) is a non-invasive brain imaging method that induces electrical currents in the brain to stimulate neural tissue. When combined with other brain imaging methods, such as electroencephalography (EEG), real-time information on cortical excitability and connectivity can be acquired. So far, TMS has been applied to several brain areas, but the combination of simultaneous TMS and EEG (TMS-EEG) is in an early stage and not many studies exist. This is due to the fact that TMS generates large artefacts in EEG which are difficult to remove with the present signal processing methods.

One of the brain areas studied with TMS is the visual cortex. The responses coming from it, however, are difficult to measure because visual processing is widely spread along the occipital lobe and no external measures, such as the motor evoked potential (MEP) arising after motor cortex stimulation, can be obtained. Due to this, TMS studies related to the visual system are mainly based on measuring the behavioural changes right after stimulation. Another used response is a phosphene, which is an artificial visual percept seen by the stimulated subject. Phosphenes are, however, very subjective as their analysis is based on each subject's own view on them.

This master's thesis covered a TMS-EEG and a TMS study with five different paired-pulse and a single pulse stimulation protocols on the human primary visual cortex. In addition, a control protocol was applied on the parietal cortex. Paired-pulse protocols are widely applied in the motor cortex, where they can be used to study the phenomenon of facilitation and inhibition of the MEPs.

1.1 Aims of the study

The study had three aims, which were:

1. to apply independent component analysis (ICA) to clean the EEG data
2. to explore the effect of different paired-pulse protocols on the TMS-evoked EEG
3. to explore the effect of different paired-pulse protocols on the amount of perceived phosphenes.

The work included the background information for the studies, the actual measurements, data analysis, and data interpretation. To the best of knowledge, no studies exist so far exploring the TMS-evoked EEG responses to different paired-pulse protocols on the human primary visual cortex. In addition, this was the first time that ICA has been applied to remove artefacts from the TMS-evoked EEG responses measured from the primary visual cortex.

2 Background

2.1 Cerebral cortex

The brain can be divided into three parts (Figure 1): the cerebrum, the cerebellum, and the brain stem. The cerebrum is the largest part of the brain and it is located at the top of the brain. The cerebellum lies under the cerebrum and is mainly a movement control center. The part that connects the cerebrum to the spinal cord is the brain stem and it functions as a controller of breathing and body temperature, among other functions. [1]

The outermost layer of the cerebrum is the cerebral cortex. It consists of four lobes presented in Figure 1: the frontal lobe, the parietal lobe, the temporal lobe, and the occipital lobe. These lobes can be further divided into functionally distinct areas, which are specialized in specific actions, such as the motor, somatosensory, and visual areas (Figure 2). The specialized areas in the cortex have a significant role in several so called higher level brain functions, such as language, memory, visual perception, movement planning and execution, attention, and conscious thought. [1]

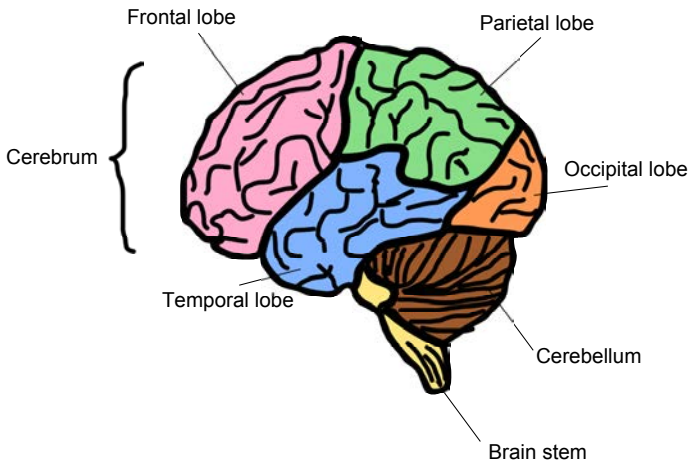

Figure 1: The three parts of the brain: the cerebrum, the cerebellum, and the brain stem. The outer layer of cerebrum, the cerebral cortex, divides into four lobes, which are the frontal, the parietal, the temporal, and the occipital lobe.

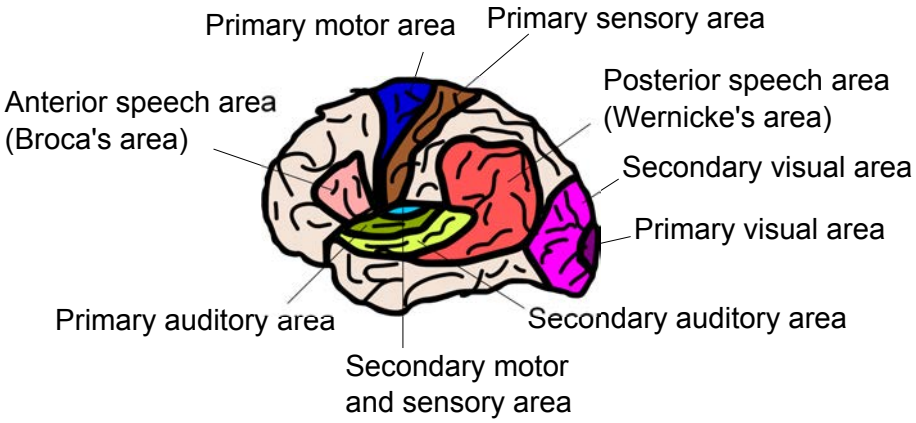

Figure 2: Some of the main functional areas in the human cortex.

The cerebral cortex is folded and wrinkled to increase the cortical surface area [1]. The grooves on the surface are called sulci, and the bumbs gyri [1]. Each cortical area consists of a characteristic sulci and gyri structure, however, some intersubject variation exists [1]. The average thickness of the cortex is small, only about 2.5 mm and it fluctuates greatly depending on the cortical region [2]. For example, the thickness of the motor cortex is 4.5 mm and the thickness of the visual cortex only about 1.45-2.0 mm [2].

The cerebral cortex includes about 16 billion neurons [2] of the total 100 billion neurons in the brain [1]. A neuron is the specialized cell of the brain (Figure 3) [3]. It is made of a cell body, which contains the nucleus of the cell and the axon, which is an electricity conducting fiber delivering information from the neuron [3]. An axon extends from the cell body to nerve terminals called synapses [3]. Synapses are the contact points which transfer information from one neuron to another [3]. The branches collecting information to a neuron from other neurons are called dendrites [3]. Dendrites form synaptic connections with the axons of other neurons [3].

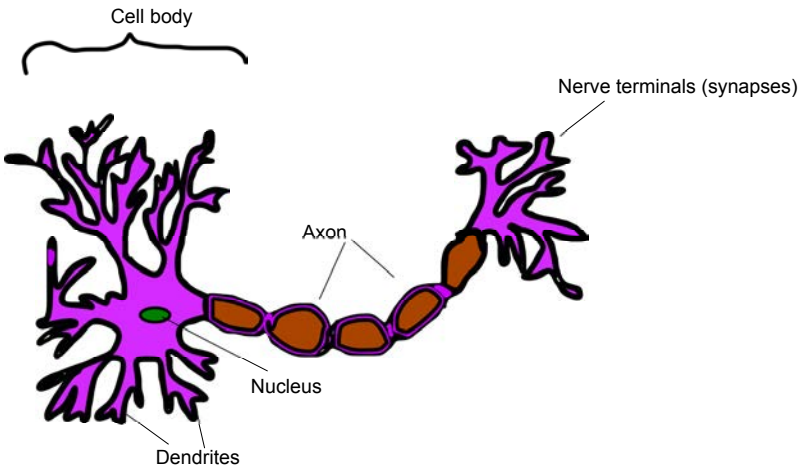

Figure 3: The structure of a typical neuron.

Neurons in the cerebral cortex can be divided into two categories based on their appearance: pyramidal and stellate neurons, presented in Figure 4. From these, the pyramidal neurons are more numerous than stellate neurons. The pyramidal cells have an apical dendrite which extends through all the layers of the cerebral cortex. The dendrites are covered with spines that provide a large surface area to form synaptic contacts. Stellate neurons, on the other hand, can also have spines but have only short dendrites and axons, and do not connect to distant sites like pyramidal neurons. Both the pyramidal and stellate neurons have several different functions, however, not all of them are known. Mainly, the pyramidal neurons are the primary excitatory units and the stellate neurons inhibitory units. [2]

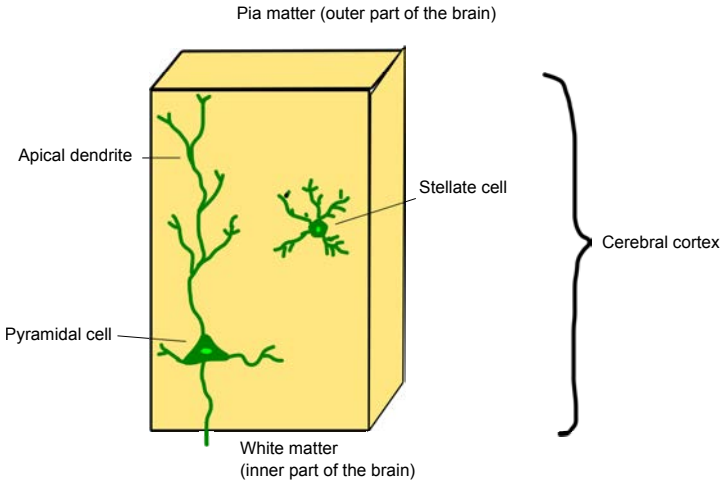

Figure 4: The two major classes of neurons in the cerebral cortex: the pyramidal and the stellate neurons.

2.1.1 Cortical excitability

The membrane potential of a neuron is defined as the instantaneous voltage across the cell membrane [1]. At rest, the inside of the cell is electrically negative in comparison with the outside of the membrane due to ion equilibrium [1]. Typically, this resting potential is about -65 mV [1]. For a nerve impulse to occur, opening and closing of water-filled tunnels in the cell membrane, called ion channels, need to occur [3]. Ions passing through the membrane generate an electrical current which produces a voltage change across the membrane [3]. If the voltage change is above neuron's excitability limit, the neuron will fire a signal called the action potential [1]. The action potential travels through the neuron's axon to the synapses and spreads to the neuronal network [1]. Each neuron is connected to the network through excitatory (depolarizing) and inhibitory (hyperpolarizing) synaptic connections [1]. The total output and the state of the neuron depend on the amounts of excitatory and inhibitory connections [1].

The cortical excitability is defined as the responsiveness of the cortex to external stimulation [4]. The momentary distribution of the neuronal network's neuron states is directly related to the cortical excitability [5]. In addition, the cortical excitability is affected by the geometry of the tissue, the availability of neurotransmitters in the synapse, and the strength of the synapses [5]. Abnormal excitability is usually related to brain disorders, such as Parkinson's disease [6], dystonia [7], stroke [8], and epilepsy [9].

2.2 Visual system

2.2.1 The eye

The processing of visual information begins in the eye (Figure 5) [10]. Eyes detect information from the visual field, which is defined as the region that can be seen with both eyes looking straight ahead (Figure 6) [1]. If this region is divided into half from the central vertical line, the region on the right is referred to as the right visual hemifield, and the region on the left as the left visual hemifield [1]. Once light from the visual field has travelled through the lens and reached the back of the eye, an image is formed on the retina [10]. This image is inverted and reversed, meaning that the upper part of the visual field is projected onto the lower retina, and the lower part of the visual field to the upper retina [10]. In addition, the right visual field is projected to the left side of both eyes, and the left visual field to the right side of both eyes [10].

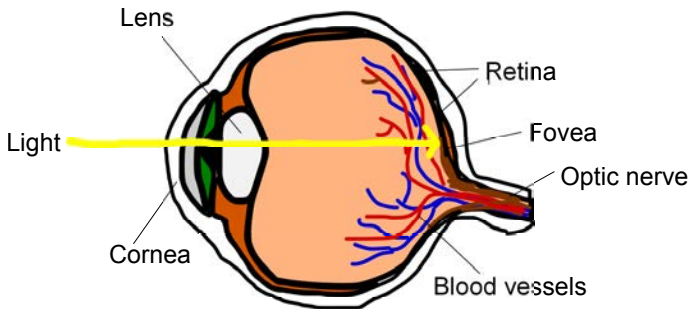

Figure 5: A simplified cross-section structure of the eye.

The point of the sharpest vision in the retina is the fovea [10]. The fovea corresponds to only one to two degrees of visual field, but it is connected to about half of the fibers in the optic nerve, and is represented by half of the cells in the primary visual cortex [10]. The optic disk is at the back of the retina [10]. The optic disk is the region where the axons leaving the eye merge and form the optic nerve [10]. The location of the optic nerve in the retina lacks of photoreceptors that are plentiful in the other parts of the retina [10]. The role of photoreceptors is to convert the electromagnetic radiation entering the eye into neural signals [1].

2.2.2 The central visual system

After the photoreceptors in the retina have extracted the visual information from the visual image, the information is transferred to the brain via a neural pathway called the retinofugal projection presented in Figure 6. This pathway consists of three structures which need to be passed before the information reaches the primary visual cortex. These structures are the optic nerve, the optic chiasm, and the optic tract. The optic nerves are located at the back of both the right and left eyes at the optic disks. The nerves pass through the fatty tissue behind the eyes and then through the holes at the floor of the skull. After entering the skull, the optic nerves from both eyes unite and form the optic chiasm which is located at the base of the brain. The optic chiasm acts as a divider, as the axons from the nasal retinas of the optic nerves cross from the left to the right side and vice versa. [1]

Following the crossovers, the axons form the optic tracts which travel under the brain's pia matter along the lateral surfaces of the diencephalon which is a structure inside the cerebrum relaying sensory information between different brain areas, among other functions. Some axons separate from the optic tract to form synaptic connections with the hypothalamus to influence a variety of biological rhythms such as the sleep and wakefulness cycle, and some connect with the midbrain to control the size of the pupil and some eye movements. However, most of the axons end up to form synaptic connections with the right and the left lateral geniculate nucleus (LGN) located in the dorsal thalamus. Both the right and the left LGN comprise of neurons that will be summed with the axons projecting from the retina to the occipital lobes where the primary visual cortex is located. The LGNs act

as a feedback loop, as about 80 % of the input excitatory synapses originate from the primary visual cortex, and in the LGN these are mixed with the connections originating from the retina, and connected back to the primary visual cortex. [1]

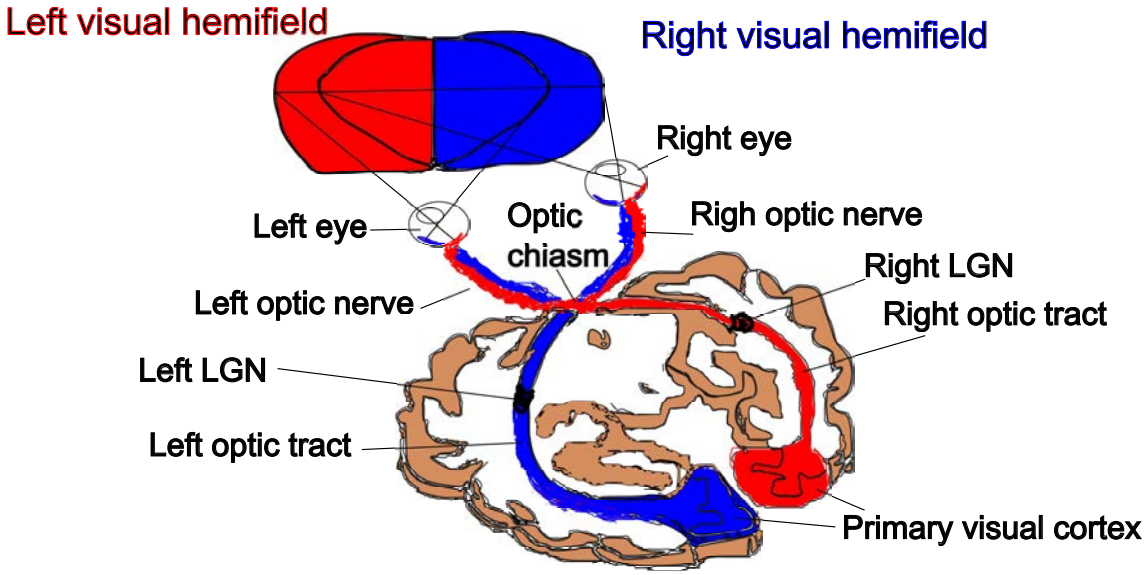

Figure 6: Structure of the central visual system.

The primary visual cortex, also known as the Brodmann's area 17, V1, and the striate cortex, is located in the occipital lobe of the brain, and is the initial place where the visual perception happens. V1 consists of several different neuronal shapes, but the two main ones are spiny stellate cells and pyramidal cells. Neurons located in V1 have binocular receptive fields, which means that they have receptive fields from both eyes. Due to this, it is possible to form a single image from two eyes. The receptive field of a neuron is the region of space in which the presence of a stimulus will influence the firing behavior of that neuron. [1]

Visual information is processed in parallel by different brain areas while following a certain hierarchy (Figure 7). After information is processed in V1, it is send to these other brain areas in the visual system. The flow of information can go either along the dorsal stream or along the ventral stream. The dorsal stream functions as an analyzer of visual motion and visual control of action, and includes areas such as V5. Ventral stream, on the other hand, is estimated to have a role in the perception of the visual world and in the recognition of objects. Ventral stream comprises of areas such as V4. When moving away from V1, the receptive fields of neurons become much more complex than in V1. [1]

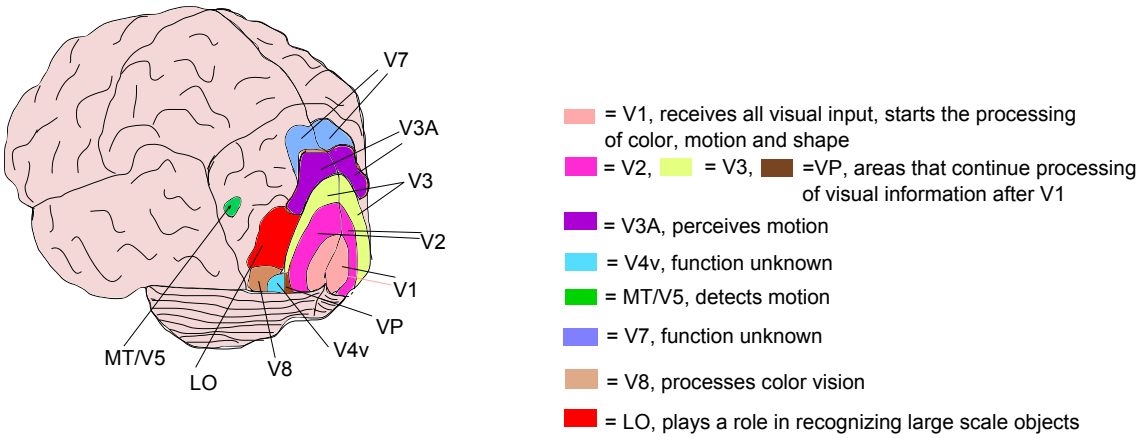

Figure 7: Areas in the visual cortex. Modified from [11].

2.3 Transcranial magnetic stimulation

The scientific enquiries in electrophysiology and electromagnetism have produced several methods that can be used to generate electric currents in nervous tissue. These include methods such as transcranial magnetic stimulation (TMS), transcranial direct current stimulation (tDCS), and deep brain stimulation (DBS) [12]. From these, TMS has become the most common in clinical applications, as it is non-invasive, painless, and has a wide range of applications, for example, in rehabilitation and intraoperative monitoring [13]. In addition, TMS can be used to study motor control, movement disorders, vision, attention, memory, speech and language processing, epilepsy, stroke, pain, depression, brain plasticity, and many others [14].

By using TMS, causal relationships between the stimulated brain area and behavior can be demonstrated. TMS can also interfere with the neuronal activity by creating a temporary disruptive effect on the brain referred to as a virtual lesion. Virtual lesions are thought to occur from the synchronization of a large proportion of neurons in the stimulation location, which induces inhibitory postsynaptic potential reducing cortical activity for 50 to 200 ms after the TMS pulse. [15]

In the following subsections, the historical background of TMS is briefly presented followed by the physics and the technological aspects of TMS. After, the biophysical effects of TMS are discussed, and lastly, the relevant applications of TMS on the visual cortex are presented.

2.3.1 Short history of transcranial magnetic stimulation

The fundamentals of TMS follow the principles of electromagnetic induction which was discovered by Faraday in 1831 [16]. Some decades later in 1874, Bartholow described a method where the bare human cerebral cortex was stimulated by electrical currents, and movements in the body were generated [17]. In 1896, d'Arsonval

placed the head of a subject in a changing magnetic field which created flickering lights in the visual field of the subject [16]. Experiments of human peripheral nerve stimulation were reported in 1965 by Bickford and Fremming. First successful transcranial magnetic stimulation and clinical studies were made in 1985 by Polson, Barker, and Freeston. These experiments led to the beginning of TMS technology, and several companies were established in the following years, such as Magstim Company Ltd, Uk and Nexstim Oy, Finland.

2.3.2 Physics of transcranial magnetic stimulation

Neural tissue can be stimulated non-invasively through the skull by applying TMS. When a TMS coil is placed on the scalp ready for a TMS pulse, a large capacitor of up to several kilovolts in the stimulator is discharged within approximately 100 μs, generating a changing current in the coil. This produces a changing magnetic field of 2 to 3 T around the coil, which induces an electric field of about 100 mV/mm [16] in the neural and non-neural tissues beneath [18]. The electric field generates an electric current which is in the opposite direction related to the current in the coil. If the amplitude of the electric current, the duration, and the direction are appropriate, neurons or their axons can be depolarized [15]. The strength of the electric field and the current in the cortex are both proportional to the rate of change of the magnetic field in the stimulation coil according to Faraday's law [16]:

$$\nabla \times \mathbf{E} = -\frac{\partial \mathbf{B}}{\partial t}, \tag{1}$$

where $\mathbf{E}$ is the electric field in the cortex, $\mathbf{B}$ the magnetic field generated by the stimulation coil, and t time. The magnetic field generated by the coil can be obtained from the Biot-Savart law [19] :

$$\mathbf{B}(\mathbf{r}, t) = \frac{\mu_0}{4\pi} I_{\mathrm{C}}(t) \oint_{\mathrm{C}} \frac{d\mathbf{l}(\mathbf{r}') \times (\mathbf{r} - \mathbf{r}')}{|\mathbf{r} - \mathbf{r}'|^3}, \tag{2}$$

where μ_0 is the permeability of vacuum, C the path of the coil windings, and dl the differencial length of the coil, in the direction of current. It must be noted that the magnetic field itself has no direct effect on neural tissue, all the effects occur due to the electric field induced by the changing magnetic field [19].

TMS is applied commonly with either a circular or a figure-of-eight coil [20]. With the circular coil the induced current in the cortex is the largest near the outer edge of the coil, and so the coil lacks of focality [20]. However, as most of the circular coils are big in diameter, they offer good penetration to the deeper parts of the cortex [20]. Figure-of-eight coils, on the other hand, are made of two circular coils placed next to each other [20]. The currents in the coils flow in opposite directions. At the junction point of the circular coils, the currents have the same direction and they summate [20]. Due to this, the figure-of-eight coil has the maximum current just below the junction giving an excellent stimulation focality [20]. However, compared with circular coils, the depth of stimulation penetration is smaller in figure-of-eight

coils as the circular coils in them are small to keep the stimulation focal [20]. Other TMS coil types also exist, such as the double-D and the H-coil, however, their use is quite rare [20]. In research and clinical applications, the figure-of-eight coil is the most used coil type [20]. Due to heating and internal repulsive forces, the shapes and sizes of coil designs are quite limited [21], and the efficiency of TMS decreases as the coil size decreases [18].

TMS pulses can be given as single pulses, as paired-pulses, or as repetitive TMS (rTMS) (Figure 8) of low or high intensity [14]. Single pulse protocol refers to single pulses given with a relatively long intertrial interval (ITI), paired-pulses to a protocol where two pulses are given with a short interstimulus interval (ISI) followed by a longer ITI before the next paired-pulse sequence, and rTMS to a protocol where TMS pulses are given rapidly with either in short trains followed by a break or in one long train [16].

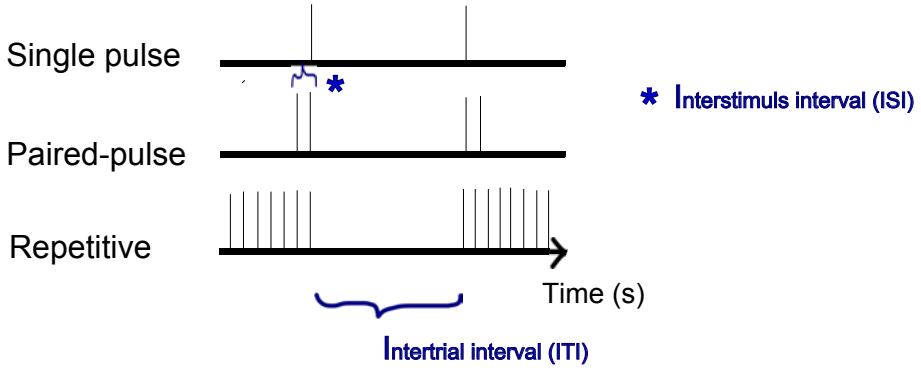

Figure 8: Different TMS pulse protocols: single pulse, paired-pulse, and repetitive TMS. Typically, the intertrial intervals are in the order of seconds, and interstimulus intervals in the order of milliseconds.

There are two typical TMS pulse waveforms, monophasic and biphasic [20]. The monophasic pulse has a magnetic field which rises sharply from zero to its peak value, and returns slowly back to zero-level [16]. The generated electric field in the brain, however, is not monophasic as it is the time derivative of the magnetic field and so, it is biphasic [16]. In the biphasic pulse, on the contrary, the magnetic field resembles one cycle of a sinusoid wave which gets damped toward the end of the pulse [16].

TMS can also be combined with other imaging methods, such as EEG, positron-emission tomography (PET), functional magnetic resonance imaging (fMRI), single-photon emission computed tomography (SPECT), and near infrared spectroscopy (NIRS) [12]. From these, the co-registration of TMS-EEG offers possibilities to study the corticocortical connectivity and brain reactivity with millisecond temporal resolution [13]. Information about the metabolic changes and brain functions can be obtained with PET [22] and SPECT [12]. fMRI, on the other hand, gives

information on which brain areas TMS has effect on and their connectivity, and by combining NIRS to TMS, the amount and the oxygen level of hemoglobin near the stimulation area can be studied [12].

2.3.3 Biophysical effects of TMS

As TMS is capable of depolarizing neurons and their axons, it can initiate action potentials and alter the level of neural excitability both during and after stimulation [18]. Action potentials of the neurons are not visible in the EEG, due to their symmetric current distribution and short duration [23], however the following post-synaptic activations in the cortex are directly seen in the EEG [24]. As the TMS induced currents in the cortex last only a fraction of a millisecond, also the effects of the TMS pulse in the EEG are quite short-term [23]. In addition, TMS may induce modifications in the membrane resting potentials and thresholds of neural tissue, membrane channel properties, and synaptic connectivity [18]. However, the mechanisms taking place in the background are still unknown [18]. What is known is that the effects are most likely maximal in the neural tissue with the highest current density below the coil, particularly at axonal boundaries and locations where fibers bend and so cause geometrical discontinuities [25]. Furthermore, several studies have shown that TMS preferentially activates the less active neurons [26], [27].

TMS also causes secondary effects on the surrounding areas and in the areas directly connected with the stimulated area [14]. Depending on the coil size, type, and relative position to the tissue, tissue distribution, and measurement paradigm, the size of the area affected by the stimulation varies greatly, and it is estimated to be around 100-200 mm^2 [18]. The efficiency of the stimulation is also affected by the orientation of individual cells, sulci, and gyri relative to the coil location and tilt. These orientations are unique in each brain, and so the optimal orientation of the electric current varies between subjects [18]. The choice of current orientation has an impact on the needed stimulation threshold, the timings of neural response latencies, differences in the resulting evoked waveforms, and the summed network effect [28]. In addition, the shape of the stimulation waveform affects the needed stimulation threshold, response latencies, and evoked waveform shape [29].

2.3.4 Phosphenes

A high intensity TMS applied to the primary visual cortex causes subjects to see phosphenes [15] that are spots of light in the visual field [14]. On the contrary, when a low intensity is used, subjects may perceive scotomas [15] that are blind spots in the visual field [14]. Phosphenes generated by the primary visual cortex are usually stationary, and those due to the stimulation of V5 are moving [14]. Phosphenes result from the direct activation of neuronal populations encoding visual input, however, the neural mechanisms underlying the generation are mostly still unknown [30].

The induction of phosphenes is strongly linked to state-dependency [31]. State-dependency means that the behavioural and perceptual effects of TMS depend upon the initial state of the neurons just before the start of the stimulation [31]. In other words, different levels of fatigue of subjects, the usage of drugs, being unfamiliar with TMS, and so forth, are all factors that affect the TMS responses [31]. Another strong factor is the current direction [32]. On V1, the optimal direction to induce phosphenes is from lateral to medial which means from left to right [32].

2.3.5 Transcranial magnetic stimulation combined with electroencephalography

By combining TMS with EEG, the excitability and connectivity of the brain can be studied non-invasively. However, due to large electromagnetic artefacts in the EEG induced by the TMS pulse, measurement is challenging and TMS compatible EEG systems need to be used. Nevertheless, even with these special systems, several artefacts may arise from the movement of the electrodes, the muscles activated near the stimulation location, eye movements and blinks, electrode polarization, the evoked somatosensory responses due to the vibration of the coil, or auditory brain responses evoked by the sound of the stimulation. To reduce these artefacts, careful precautions in the stimulation process need to be considered. [23]

2.3.6 Paired-pulse protocols

Studies utilizing short-interval paired-pulse TMS protocols have given important information on the physiology of the human motor cortex [33]. By changing the ISI between the two pulses, either intra-cortical facilitation (ICF) or intra-cortical inhibition (ICI) can be seen on the MEP [34]. With ICF it is meant that the response to the second pulse is larger in relation to the response to the first pulse and with ICI that the response to the second pulse is smaller [34]. The first stimulus is called the conditioning stimulus (CS) and its role is to activate cortical neurons [15]. The second stimulus is called a test stimulus (TS) and it is used to test the excitability of the cortex [15]. When ISI used is smaller than 5 ms, the effect on the motor cortex is inhibitory and when ISI is between 8 and 30 ms, the response is facilitated [15]. The effects of long ISI has also been studied on the motor cortex [35] [36]. If the ISI is between 100 and 250 ms, the induced effects in the MEPs are inhibitory [35] [36].

The phenomena of facilitation and inhibition in the motor cortex are assumed to be related to the excitability of separate interneuronal circuits [37] [38] [39]. Similar occurrence of facilitation and inhibition has been discovered from parietal [40] and prefrontal cortex [41]. To investigate whether the same phenomena of facilitation and inhibition also exist in the visual cortex, Sparing et al. studied cortical excitability with phosphenes using short ISI paired-pulse protocols similar to in studies made on the motor cortex [34]. On the visual cortex, the number of phosphenes perceived after a defined number of TMS pulses at a certain intensity [42] [43] [44], as well as the phosphene threshold (the smallest TMS intensity evoking phosphenes) have been demonstrated to be reliable measures of the cortical excitability [45] [46].

As the mechanisms of generation and origin of phosphenes are not fully known, Sparing et al. made a hypothesis that if similar facilitation and inhibition patterns would be found related to phosphenes, more information about the physiological mechanisms of phosphene generation could be revealed [34].

In Sparing's study, it was found that contrary to the results on the motor cortex, on the visual cortex all the short-interval paired-pulse protocols with 2,3,8, and 12 ms ISI facilitated the perception of phosphenes [34]. No inhibitory effects were found with short-interval ISIs [34]. The stimulation intensities were adjusted for each subject so that the first pulse was given with an intensity of 90 % of the measured phosphene threshold and the second pulse with the phosphene threshold [34]. These results suggest that the mechanisms related to phosphene generation are different from facilitation and inhibition mechanisms discovered on the motor cortex with short ISIs [34]. The differences might be explained by the fact that the motor and visual system are functionally different, in other words the motor system functions in body movements and the visual cortex in visual sensations [47]. In addition, the output responses of the systems differ, as MEPs are measurable signals and phosphenes are subjective sensations [47].

2.3.7 Phosphene studies employing TMS-EEG

The temporal evolution of a TMS-evoked potential related to phosphenes has been studied by Taylor et al. They applied single pulse TMS on the primary visual cortex. It was found that phosphene perception is linked to the late components of evoked potentials between 160 and 200 ms after the TMS stimulation. In addition, it was discovered that the perception of phosphenes is a widespread phenomenon, and it arises from extensive cortical processing between a large range of visual areas. [30]

The influence of cortical excitability on phosphene induction has been studied by Romei et al. They found that whether or not a phosphene is perceived can be predicted from the cortical excitability just before the TMS pulse. This result suggests that the inherent variability in the cortex affects the differences in phosphene perception in consecutive TMS trials. [48]

3 Methods

3.1 Subjects

Twelve healthy subjects (9 males and 3 females) aged from 23 to 43 (mean = 29.3) years participated in the TMS-EEG study. All the subjects gave their written informed consent before participating, and the study was approved by the Ethics Committee of Helsinki University Central Hospital. In addition, all the subjects were screened for their suitability to be stimulated with TMS. Eleven of the subjects were right-handed and one left-handed. All the subjects had normal or corrected to normal vision. Due to poor data quality, one subject was excluded from the

analysis. From eleven included subjects in the main experiment, five (2 males, 3 females) participated in the follow-up TMS experiment. Six of the subjects had previous experience in being a subject in phosphene studies. With the exception of two people (thesis author and instructor), the subjects were naive to the goals of the study.

3.2 Experimental design of TMS-EEG experiment

The subjects were seated comfortably on Nexstim's reclining TMS stimulation chair and given a standard laptop with a matte screen on their lap (Figure 9). The distance between the subject and the laptop screen was about 50 cm. All the lights in the room were darkened and the only light source was the dark screen. The task of the subjects was to focus on a fixation cross presented near the left edge of a black screen. The position of the laptop was adjusted so that the fixation cross was in the center of the visual field of the subject. The reason for using the left edge for the fixation cross was that in case the subjects saw phosphenes, they were in the right visual field. This was because the stimulation location was in the left primary visual cortex. Having a wide dark background in the right visual field assisted the subjects in seeing phosphenes. In addition, by having a fixation cross, unnecessary eye movements were minimized. Subjects were instructed to keep their head in place during the stimulation to keep the stimulation location constant and to avoid movement artefacts in the EEG. In addition, subjects were asked to avoid eye blinks, if possible, right after the TMS pulse. To decrease the neural responses to coil click, subjects wore ear plugs.

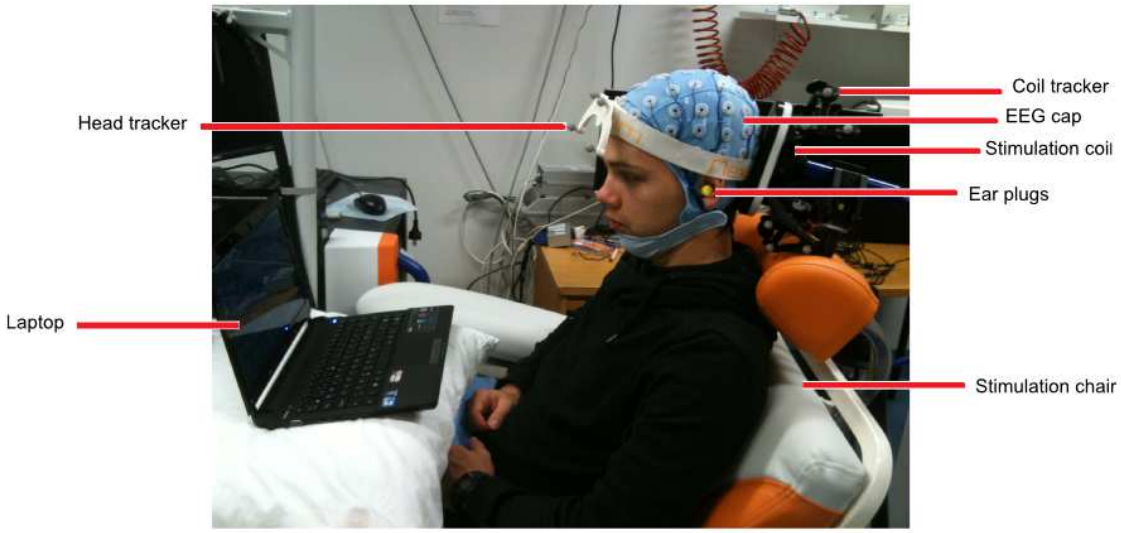

Figure 9: Experimental setup.

Before the main experiment, high intensity (80 % of the maximum output of the stimulator) biphasic TMS pulses were given to find the phosphene hot spot from the left primary visual cortex. The hot spot was defined as the location where the

subjects saw the most phosphenes with their eyes closed. If such a spot was found, it was used as the stimulation location in the actual experiment. If subjects did not perceive any phosphenes, stimulation was targeted left from the inion, which is a typical location for seeing phosphenes (Figure 10). The inion is the external bony projection of the occipital bone [49].

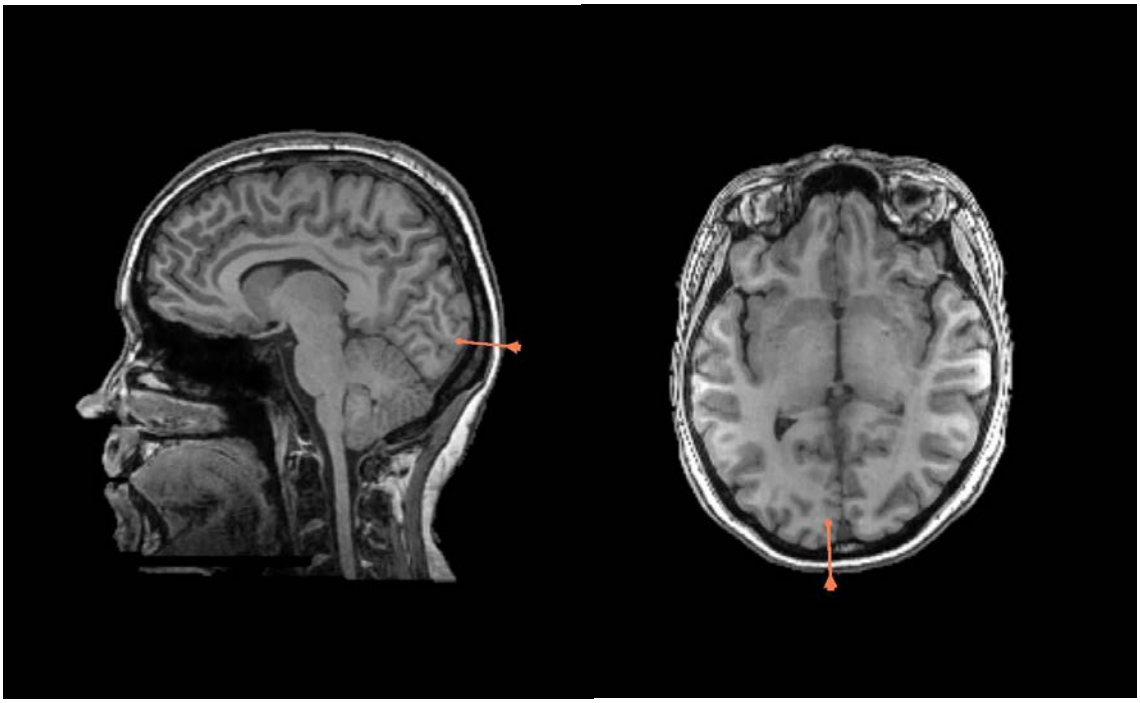

Figure 10: A stimulation location presented in a magnetic resonance image (MRI).

After finding the phosphene hot spot, the intensity of the stimulation was adjusted for each subject by using MOBS software [50]. MOBS uses a modified binary search paradigm, which sets different TMS stimulation intensities, and based on the obtained results (subject perceived a phosphene or did not perceive), the phosphene threshold is calculated. The upper limit of the stimulation intensity was adjusted to be 80 %, as with higher intensities the monophasic TMS stimulation begins to be uncomfortable for the subject. The average phosphene threshold was 58 % (approximately 72 V/m in the neural tissue). If a subject did not perceive phosphenes, the intensity of 80 % was used (approximately 105 V/m in the neural tissue). Subjects reported whether they perceived or did not perceive a phosphene verbally after each TMS pulse.

In the main experiment, seven stimulation protocols were used. The monophasic TMS pulses were delivered with the Nexstim eXimia TMS stimulator using a figure-of-eight coil. Protocols included five paired-pulse TMS with 10 ms, 30 ms, 50 ms, 70 ms, and 90 ms ISI, single pulse, and control. In the paired-pulse protocols both the pulses had the same intensity. In addition, in all the protocols the intensity was the

same. Paired-pulse and single pulse protocols were given to the phosphene hot spot determined previously or to the standardized location next to inion. The control protocol was a single pulse TMS applied on the parietal cortex, lateral to the centro-parietal electrode CPz. The cortical area under CPz has not been reported to be linked with phosphenes, MEPs, or the control of visual spatial attention [30], and so it was suitable for a control in the study. A control was used to gain information on what part of the TMS-evoked potentials was specific to the primary visual cortex and what might be an artefact. Each protocol included 60 trials and the ITI was 3334 ms (Figure 11). The order of the stimulation protocols was random to avoid order effects. In the main experiment, during the ITI the subjects reported the phosphene perception by raising their right hand fingers: if a phosphene was perceived, the fingers were lifted up, if not, the fingers were left at rest.

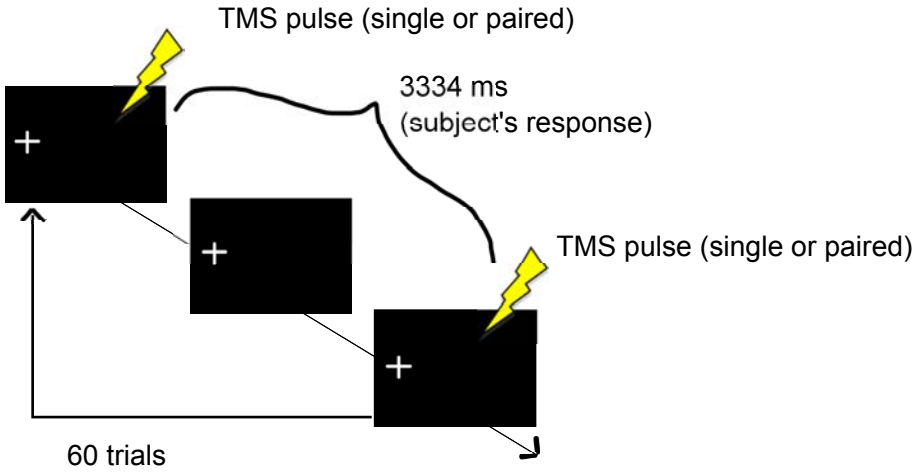

Figure 11: The experimental paradigm of TMS-EEG and TMS experiments. Subjects were stimulated either with single pulse or paired-pulse TMS, depending on the protocol. After each stimulation, there was an ITI of 3334 ms before the next TMS pulse. During this time, the subject responded whether a phosphene was perceived or not. One trial comprised the TMS stimulation and the ITI. Each stimulation protocol included 60 trials.

During the main experiment, EEG was recorded by using a 60-channel Nexstim eXimia EEG device (Nexstim Ltd., Helsinki, Finland). The ground electrode was placed on the zygomatic bone and all the signals were referenced to the right mastoid (Figure 12). The vertical eye movements, in other words, the vertical electrooculography (EOG) was recorded. The EEG data was digitized at a sampling rate of 1450 Hz. The electrode impedances during the measurement were kept below 10 kΩ. In an ideal situation, the impedances should be below 5 kΩ, however, due to the limited number of different EEG caps, for some subjects the caps did not fit well which increased the impedance.

The experimental design in the follow-up TMS experiment was the same as in the main TMS-EEG experiment. In addition, the stimulation intensities for each

subject were the same as in the TMS-EEG experiment. However, EEG was not recorded. The reason why the follow-up TMS experiment was done, was to compare the results of amounts of phosphenes seen with the EEG cap on and without.

In the course of the measurements, the TMS coil heated up quite quickly. Due to this, after each stimulation protocol the coil had to be cooled down. In total, the TMS-EEG experiment lasted approximately 3 hours and the TMS experiment 2 hours.

Figure 12: The locations of the reference and ground electrodes.

3.3 Equipment

3.3.1 TMS equipment

TMS stimulation was performed by using Nexstim eXimia TMS stimulator with the Nexstim eXimia NBS (Navigated Brain Stimulation) System (Software version 3.2.1) and with a monophasic coil (Figure 13). The equipment is manufactured by Nexstim Oy, which is a Finnish company founded in Helsinki in 2000. The company is built from the ideas developed at the BioMag laboratory of the Hospital district of Helsinki and Uusimaa in the mid 1990s.

Nexstim's NBS system is based on MRI aided navigation. The software creates a 3D-model of the head from individual MR images. The desired stimulation location can be determined from the model, and after, the model is registered to the subject's head by using a special tracking system. This way the stimulation in the subject's head can be related to the real anatomy and more precise stimulation can be done. The NBS software marks each stimulation location with the electric field parameters to the 3D model of the head. The strength of the electric field at the target is calculated using a spherical head model. The electric field direction is shown as a red-blue arrow.

Nexstim's TMS offers several stimulation modes; single pulse TMS (monophasic and biphasic pulses), paired-pulse TMS (monophasic pulses), and repetitive TMS (monophasic and biphasic pulses). Only figure-of-eight coils are available. TMS stimulation can be combined with electromyography (EMG) measurement to investigate the TMS evoked muscle responses. In addition, the system can be used with the Nexstim eXimia EEG equipment to measure the TMS-evoked EEG responses. More detailed information on the TMS-equipment can be found in Appendix A, Table A1.

Figure 13: The TMS stimulator and a figure-of-eight monophasic coil with coil trackers.

3.3.2 EEG equipment

For the recording of EEG Nexstim's eXimia EEG device was used. It has 60 monopolar electrodes for the EEG (Figure 14) and two bipolar electrodes that can be used either for vertical or for horizontal EOG, and ground and reference electrodes. All the electrodes are passive as only passive electrodes can withstand the application of TMS. EEG electrodes are mounted into a cap according to the international 10-20 system [51]. This system is used worldwide for placing EEG electrodes on the scalp and for connecting the inner cortical structures to external skull locations [52]. In studies utilizing TMS, the 10-20 system has been used for positioning the coil as the system describes electrode locations with relative distances between cranial landmarks, such as nasion and inion, over the surface of the head [52].

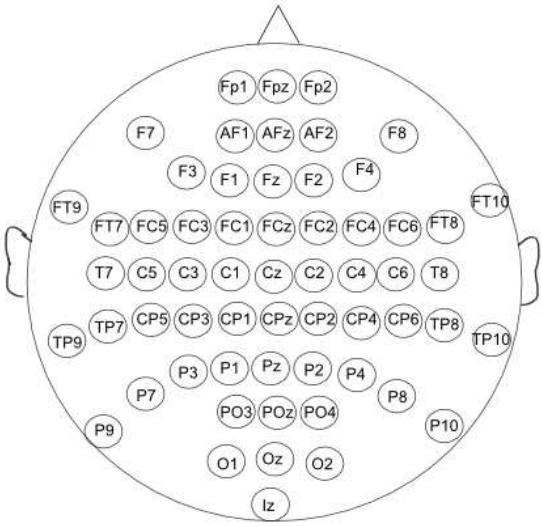

Figure 14: The electrode placement used in the study (according to the International 10-20 system).

To avoid TMS-related artefacts in the data, the system uses a sample-and-hold circuit designed by Virtanen et al. in 1999 [53]. This slew-rate limiting pre-amplifier combined with adjusted sensitivity and operational range blocks most of the artefact caused by the TMS pulse [53]. Without the use of any artefact minimising or blocking algorithm, the TMS-artefacts totally disrupt the data [23].

3.4 Data analysis

EEG data analysis was done offline using Matlab (The Mathworks, Inc. Natick, Massachusetts, USA). Some of the used analysis scripts were from Fieldtrip [54], and the rest made by the author. The data was first bandpass filtered between 0.1 and 350 Hz by applying a FIR filter to preserve phase information. Then the data was segmented into trials of 1.1 seconds (0.1 second pre-stimulus and 1 second post-stimulus). The zero-point was either at the start of the single pulse or at the second of the paired-pulses depending on the protocol. Then the concatenated data was baseline corrected by removing the mean of the signal from every data point. After this, the data was browsed visually and bad electrodes were interpolated from their neighbouring electrodes. A bad electrode was defined as an electrode which had lots of artefacts, or was loose. On average, only one to two electrodes were interpolated from each dataset.

TMS stimulation near the neck muscles generates large muscle artefacts that are several times larger than brain signals. To identify and extract these artefacts from the EEG, independent component analysis (ICA) is a suitable tool for offline processing [55]. It has already been used in TMS-EEG studies to reduce artefacts from the TMS-evoked EEG resulting from M1, the posterior parietal cortex, the

postcentral gyrys [56] [57], as well as from the dorsal premotor cortex and Broca's area [58]. To the best of knowledge, it has not yet been used with EEG recorded from the primary visual cortex.

The idea behind ICA is to extract statistically independent sources from the EEG by trying to find the linear projections from the data [55]. This can be done by maximising the mutual independence of the projections [55]. These linear projections are the artefactual and brain signal components, which mix to result in the signal recorded at the scalp electrodes [55]. The ICA algorithm assumes that the source signals are statistically independent, the mixing of the source signals at the electrodes are linear, and that the source signals and the mixing process are stationary [55]. In addition, only up to one of the source signals can be Gaussian [55]. In TMS-EEG studies, the artefacts and brain signals are generated by the same TMS pulses, however, they are still considered as independent sources with no mutual interaction. Therefore it is thought that ICA is suitable for being used with TMS [59] [60] [60] [61].

ICA has some limitations [62]. For example, the order of the components is random in each run and the energies and signs of the components are unknown [62]. However, recently a modified version of ICA was published by Korhonen et al. where the components had the same order in every run [58]. This modified version is not yet in general use, though. ICA is also very subjective, as the user needs to decide from the independent components which are artefactual and which are brain signals.

There are several different algorithms for ICA, such as Infomax, FastICA, and JADE, however, they are all based on the same definition shown in equation 3:

$$x(k) = \boldsymbol{A}s(k), \tag{3}$$

where $x(k)$ are the measured signals at time points k, $\mathbf{A}$ is the mixing matrix and $s(k)$ are the source signals. The aim is to estimate the mixing matrix and the source signals from the measured signals. The detailed description of the mathematics behind ICA can be found for example from [63].

The artefact removal algorithm used in the present study was a modified version of FastICA manual method implemented by Korhonen et al. [58]. The modification made to the algorithm was that all the trials were supplied to the algorithm separately and not as a grand average as in the article.

When using ICA, the decision between an artefactual and a real EEG component was based on the waveform, topography and the frequency contents of the independent components. An independent component (IC) was classified as an artefactual component if it was rapidly oscillating right after the TMS pulse, its amplitude was clearly higher than in normal EEG (the amplitude of EEG is typically less than 30 μV), its frequency contents were not typical of EEG (EEG normally has only frequencies below 50 Hz), or the component's topography was either centered at

frontal areas near the eyes or directly under the stimulation location.

After artefact removal, the data was browsed visually and averaged, and the pre- and post-ICA averages were compared to ensure that not too much of real EEG or too little artefactual data was removed. The data was again zero-phase bandpass filtered to preserve phase information with a 4th order Butterworth filter between 0.5 and 45 Hz. The filtering limits were changed to remove the remaining artefacts. The upper passband limit was decided based on general EEG analysis guidelines [64].

The following analysis after ICA focused on the short-lasting TMS-evoked potentials and their mean amplitude and frequency characteristics. The analyses were done for all the subjects as a group, due to a small number of subjects. On the motor cortex, the peak amplitudes have been reported depending nonlinearly on the stimulation intensity [65], and due to this, the mean amplitudes were chosen, as the subjects were stimulated with different intensities. No long lasting effects were analyzed as the recharging of the TMS caused a massive artefact 1 s after the onset of the paired-pulses and this made the data totally unreliable for analysis. The interval from the pulse onset to the artefact was too short for any long-lasting effect analysis, such as time-frequency analysis, as the frequency resolution would have been too imprecise.

3.4.1 Facilitation and inhibition in the TMS-evoked EEG responses

Whether the paired-pulse protocols caused facilitation or inhibition in the TMS-evoked EEG responses was analyzed with the two-tailed paired t-test, the repeated measures analysis of variance (ANOVA) and by looking qualitatively at the cumulative curve area and cumulative power. The data was the mean of the electrodes PO3, POz, O1, and Oz. Both the two-tailed paired t-test and the repeated measures ANOVA are statistical tests which measure whether the means of different sample groups are the same or different [66]. Single pulse condition on the primary visual cortex presented in Figure 15 was used as a baseline for the analysis. In the two-tailed paired t-test and the repeated measures ANOVA the mean amplitudes of paired-pulse protocols were compared one by one with the mean amplitudes of the single pulse condition in 20 ms time windows to reach fine temporal resolution. For the p-value to be significant, a value less than 0.05 was required. Results were corrected for multiple comparisons with the criterion that at least two consecutive time windows should have a significant p-value. This criterion was adopted from a previous TMS-EEG study on the primary visual cortex by Taylor et al. [30]. The control protocol was not included in the analysis.

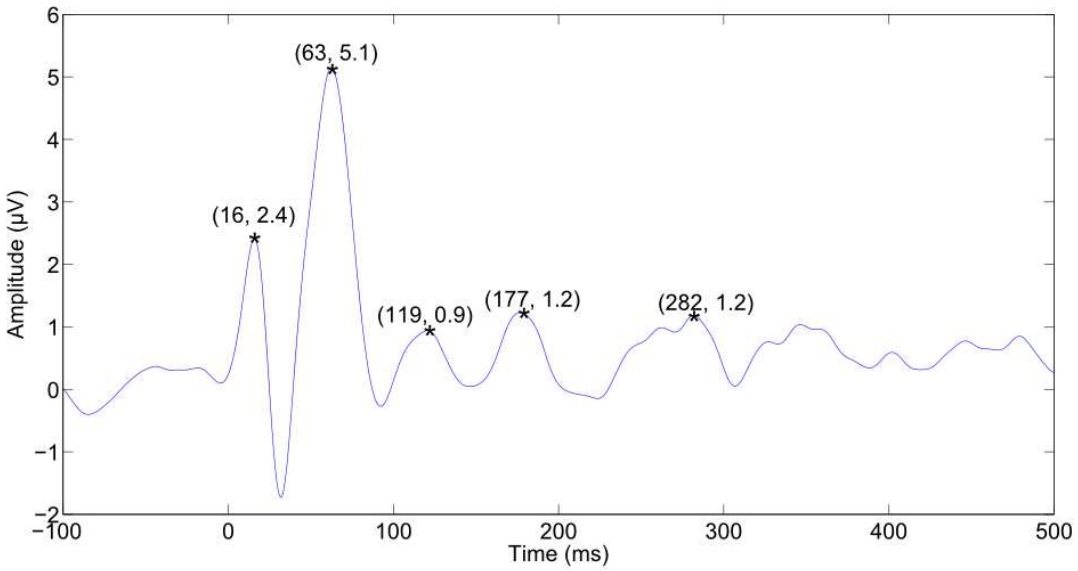

Figure 15: EEG activity following a single pulse TMS to the left primary visual cortex. The values in the brackets indicate the peak locations (time, amplitude). The TMS pulse was given at t=0.

Both the cumulative curve area and power were calculated continuously at each time point between 50 ms after either the onset of the single pulse or the second of the paired-pulses, and 500 ms. Reason for the delayed beginning of the analysis was that after 50 ms it was sure that the TMS-artefact would not influence the data any longer. Only explorative data analysis was done to gain information on the behaviour of the data. The control protocol was included in the analysis.

3.4.2 TMS-evoked phosphenes

The analysis of TMS-evoked phosphenes was based on the phosphene perception of the subjects in the TMS-EEG and the TMS experiment. The number of phosphenes per stimulation protocol were counted, and in addition the frequency and expression of phosphenes were analyzed. By the expression it was meant how the subjects experienced the phosphenes. Out of twelve subjects, five reported seeing phosphenes. However, two were excluded from the analysis as the other saw only one phosphene and the other reported seeing flashes with a frequency and expression which did not respond to normal phosphene perception. The accepted appearance of phosphenes was momentary bright spots or circles in the right visual field, contralateral to the stimulation area. The accepted frequency of the phosphenes was that the phosphenes should appear every now and then, not after each TMS pulse.

3.4.3 Cumulation effects

By analyzing the cumulation effects in the TMS-evoked potentials, the aim was to explore whether the time between consecutive trials was long enough, or was there

a possible cumulative component in the TMS-evoked potentials that was actually a remainder from the previous trials. This was analyzed by dividing the data from all the protocols into three parts: trials 1-20, trials 21-40, and trials 41-60. These sets of data were compared by mean amplitude by taking 20 ms time windows between 0 and 480 ms. The cumulation was assessed with the two-tailed paired t-test by comparing trials 1-20 with trials 21-40, trials 1-20 with trials 41-60, and trials 21-40 with trials 41-60. The analysis was done with several t-tests and not with ANOVA to gain more information on where the possible differences were. In order the cumulation to be significant, two consecutive time windows were required to have a p-value less than 0.05.

In addition, the frequency contents of each trial were averaged to study the trends in frequency. In the analysis delta, theta, alpha, and beta bands were calculated by taking the Fourier transform of the data between 0 and 480 ms. It needs to be noted that due to this short time window the frequency resolution was 2 Hz, so results were approximate and could only be used to evaluate trends. The used frequency bands were also slightly changed from standard to respond better to the frequency resolution (delta 0-4 Hz, theta 4-8 Hz, alpha 8-14 Hz, beta 12-26 Hz). As some of the subjects had more artefacts towards the end of the protocols, only 50 first trials were included in the analysis to get more accurate results.

3.4.4 Spatial spreading of the TMS-evoked EEG potentials

The spatial spreading of the TMS-evoked potentials was analyzed to gain information on how the potentials spread from the stimulation point to surrounding areas. The analysis was done with EEG scalp maps and with the two-tailed paired t-test of mean amplitude in three different brain areas: right occipital lobe, dorsoprefrontal cortex, and motor cortex (Figure 16). In scalp maps, the mean amplitude of each electrode was calculated in 20 ms time windows and presented as a mean amplitude map between 0 and 480 ms. All the protocols were analyzed separately. The data between the electrodes was interpolated from the neighbouring electrodes. The location was defined approximately as either posterior (the back of the head), parietal (the top of the head, in the back), frontal (in the front of the head, in the top), temporal (on the sides of the head, near the ears), central (central part of the head, on top), or their combination. When looking at the results of the scalp maps, it needs to be noted that the scalp maps are not showing the source signals. In other words, they do not show the areas where the signals are coming from, but how the signals behave when they reach the scalp. Control protocol was included in the analysis.

In the two-tailed paired t-tests the mean amplitudes of different paired-pulse protocols were compared with the single pulse protocol in 20 ms time windows from 0 to 480 ms. Results were considered significant if at least two consecutive windows had a p-value less than 0.05. The control protocol was not included in the study.

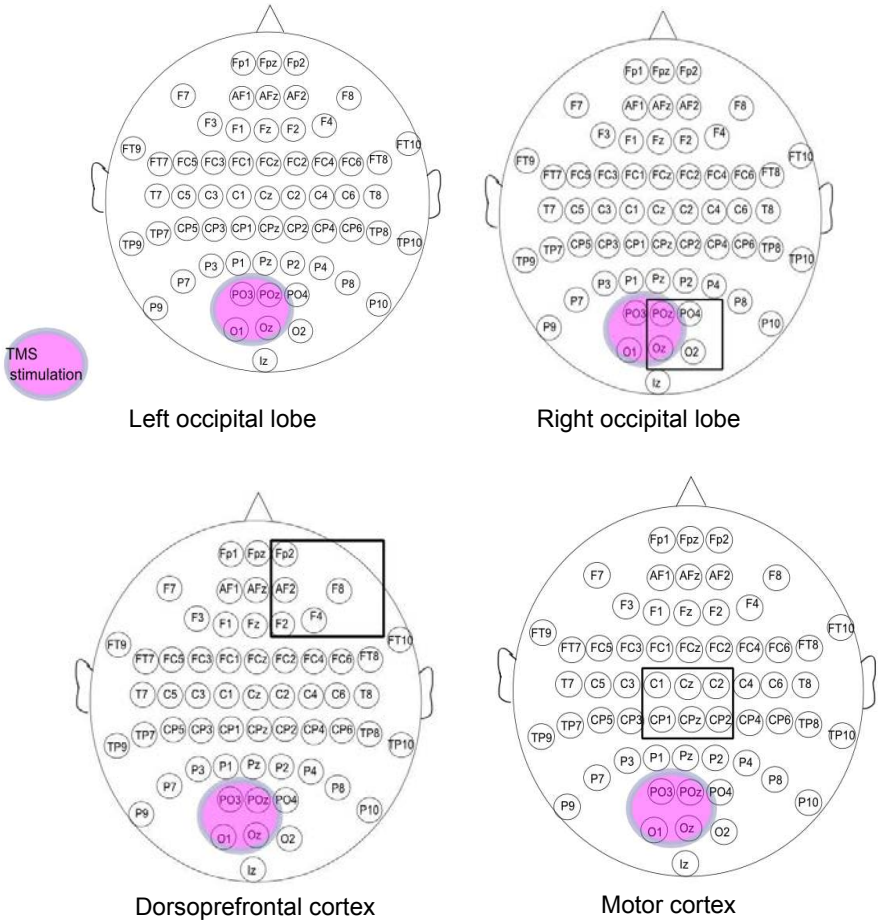

Figure 16: Regions used to analyze the spatial spreading of the TMS-evoked EEG responses. The regions are marked with a black rectangle. The left occipital lobe on the top left was the location of the stimulation (not included in the analysis).

3.4.5 Frequency contents of the TMS-evoked potentials

As the time-frequency analysis could not be done on the data due to a too short interval between consecutive trials, the frequency content of the TMS-evoked potentials were evaluated. This was done by taking the Fourier transform between 0 and 900 ms from the shifted data (zero point either at the single pulse or at the second of the paired-pulses). With 900 ms time window, the frequency resolution was 1.1 Hz. The power content of the delta (0.5-4 Hz), theta (4-7.5 Hz), alpha (8-13 Hz), and beta band (14-26 Hz) were calculated from each trial and averaged for each subject [67]. For each frequency band, two-tailed paired t-tests were done to compare the differences between the paired-pulse protocols and the single pulse protocol on the primary visual cortex. For the differences to be significant, p-values less than 0.05 were accepted. The data for the analysis was taken as the average of electrodes PO3, POz, O1, and Oz which were under the stimulation spot.

4 Results

4.1 Artefact reduction

The amplitudes of the muscle artefacts in both the single and the paired-pulse stimulation of the primary visual cortex were considerably larger than the amplitude of the EEG signal, as can be seen from Figures 17 and 18 (single subject, single trial). The artefacts lasted for tens of milliseconds, and ruled out the analysis of the EEG during their occurrence.

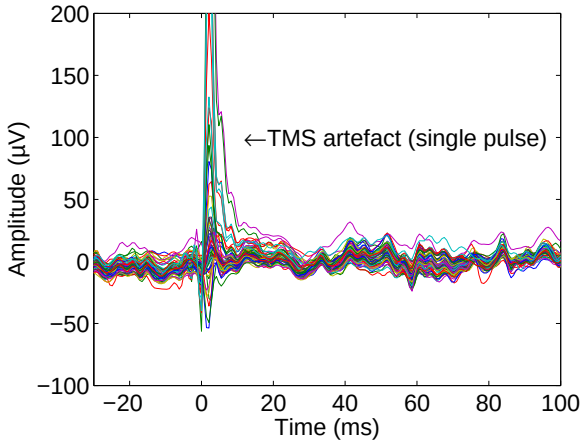

Figure 17: A typical waveform of a TMS-evoked artefact after single pulse stimulation of the primary visual cortex (data includes all 60 channels).

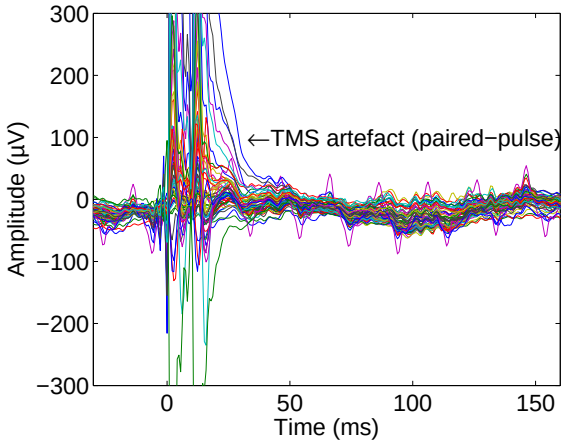

Figure 18: A waveform of a TMS-evoked artefact after the paired-pulse (ISI 10 ms) TMS of the primary visual cortex (data includes all 60 channels).

Figure 19 shows the comparison of EEG data from a single trial from a single subject before and after it was corrected with ICA. The results before ICA are presented on the left and the same data after ICA on the right. As can be seen, the artefact removal was successful in the EEG arising from the paired-pulse (ISI 10 ms) (a and b) and single pulse protocol (c and d) on the primary visual cortex. With the control protocol (e and f), some artefacts were still present after ICA, however, the areas to be used in the main analysis directly under stimulation location were nearly artefact free.

4.2 Facilitation and inhibition in the TMS-evoked EEG potentials

TMS-evoked potentials from the paired-pulse protocols are plotted along with the single pulse protocol in Figure 20. The results from the two-tailed paired t-test can be found in Appendix B, Table B1 and the F- and p-values from the repeated measures ANOVA in Appendix C, Tables C1, C2, C3, C4, and C5. As can be seen from the p-values, no significant differences were found.

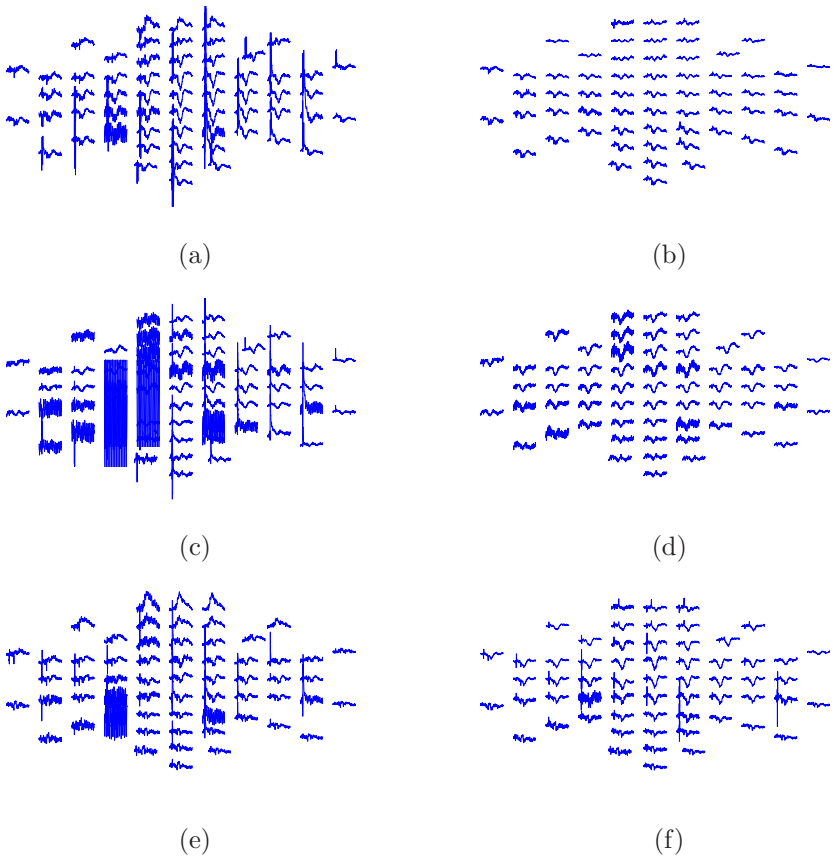

Figure 19: The TMS-evoked EEG responses from a single trial (from the same subject). Data before ICA on the left and data corrected with FastICA on the right. EEG arising after a paired-pulse (ISI 10 ms) TMS from primary visual cortex (a) and (b), after single pulse TMS from primary visual cortex (c) and (d), and after single pulse TMS from the control area left from electrode CPz (e) and (f). Data is presented in a time window from -10 to 200 ms.

The cumulative curve area and the cumulative power are presented in Figure 21 and Figure 22, respectively. As can be seen from Figure 21, the paired-pulse protocol with 10 ms ISI had the largest cumulative area when compared with the baseline, which was the single pulse protocol. In addition, approximately after 250 ms, all the paired-pulse protocols exceeded the cumulative area of the baseline. The control protocol exceeded the baseline approximately at 300 ms.

In the cumulative power of the protocols (Figure 22), only paired-pulse protocols with an ISI of 10 ms and 90 ms had greater power than the baseline protocol. Other protocols, including control, had either lower or equal cumulative power.

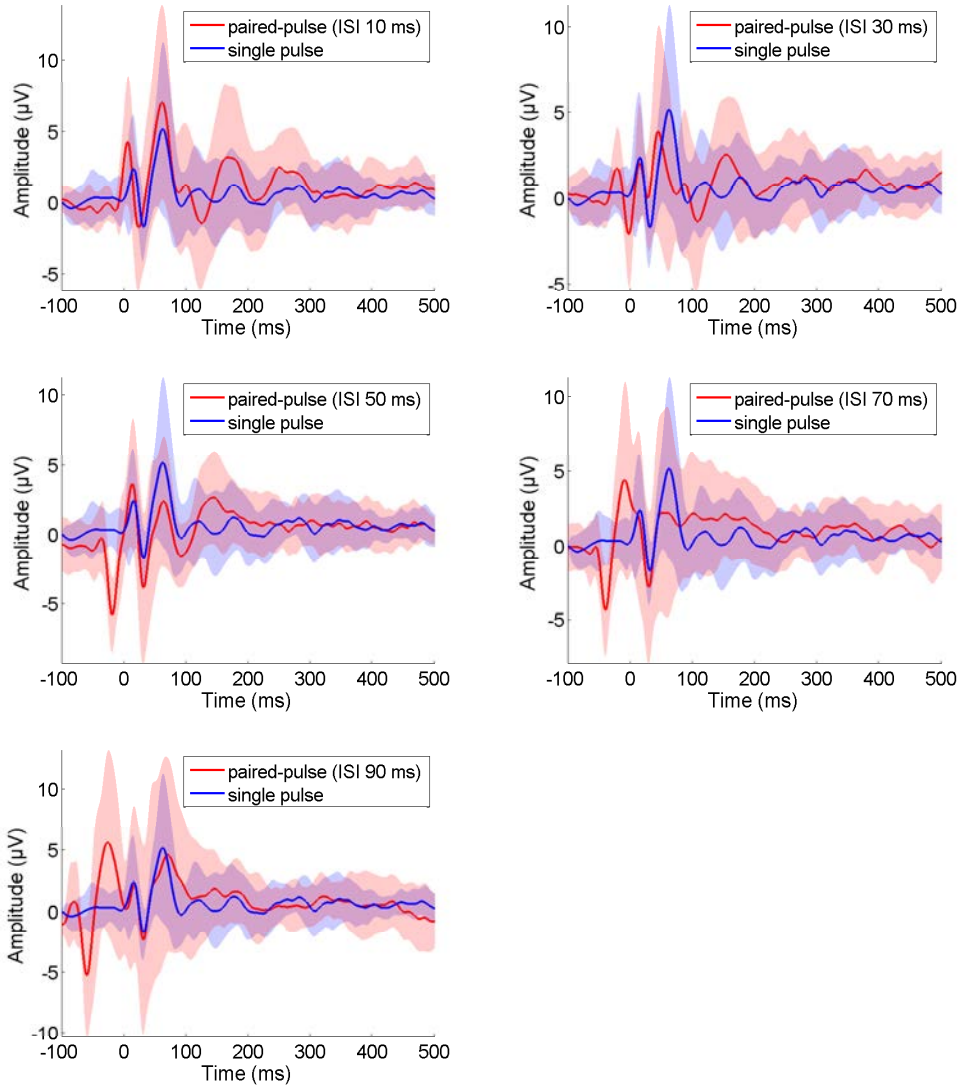

Figure 20: The paired-pulse protocols plotted along with the single pulse protocol. The faint curves represent the intersubject variation (± 1 standard deviation).

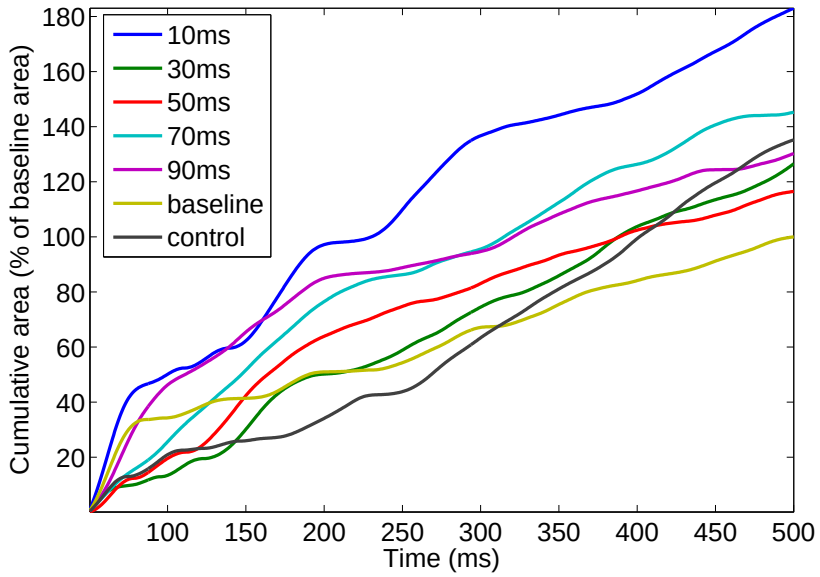

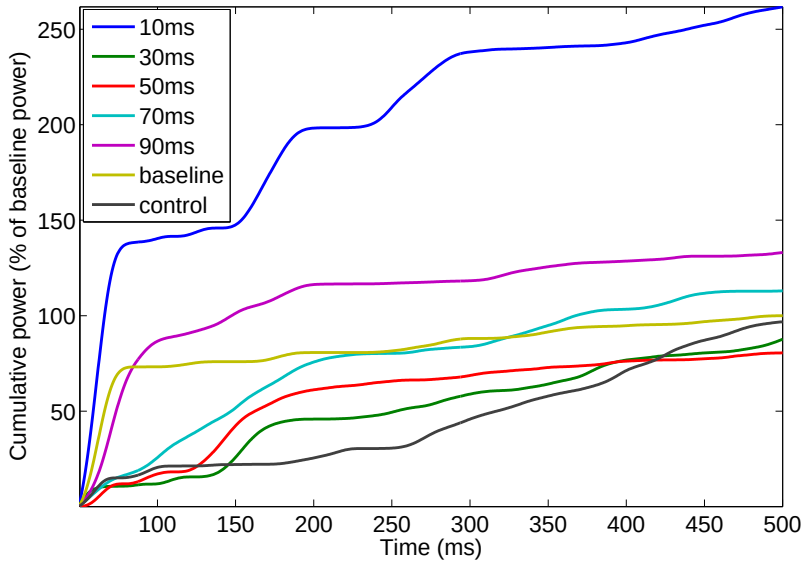

Figure 22: The cumulative power in each protocol as a percentage of the baseline power. The used baseline protocol was the single pulse.

4.3 TMS-evoked phosphenes

A large number of stimulated subjects did not perceive any phosphenes in the experiment. In total, only 3 out of 12 perceived phosphenes reliably in the TMS experiment, and 2 out of 12 in the TMS-EEG experiment (Figure 23). All the subjects in the phosphene analysis were characterized by having previous experience on phosphene studies. Due to the lack of subjects perceiving phosphenes, no statistical analysis could be done and the paired-pulse conditions were analyzed only qualitatively. As can be seen from Figure 23, more phosphenes were perceived in the absence of an EEG cap when the coil could be placed directly on the scalp. In addition, when comparing the results of the paired-pulse protocols with the single pulse, the short ISIs (10 ms, 30 ms) seemed that they may have facilitated phosphene perception and the longer (50 ms, 70 ms, 90 ms) may have inhibited it. The results from the TMS-EEG seemed to be very unclear and inconsistent and no possible trends could be seen.

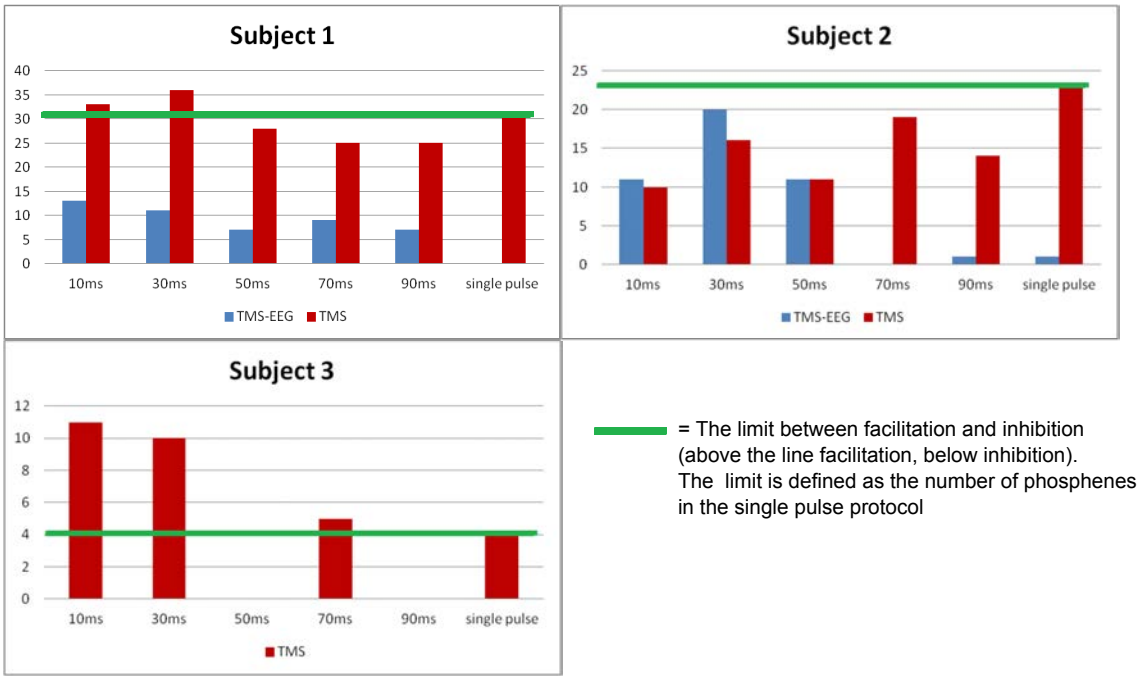

Figure 23: The number of perceived phosphenes in different protocols from three subjects. The results are shown from the TMS-EEG measurement and from the TMS measurements. In the figures, the vertical axis shows the number of phosphenes and the horizontal axis the used stimulation protocol (the ms-values indicate the ISI of the paired-pulse protocol)

4.4 Cumulation effects

The TMS-evoked potentials divided into sets of trials 1-20, trials 21-40, and trials 41-60 are presented in Figure 24 for each protocol. The p-values from the two-tailed paired t-test of mean amplitudes are presented in Appendix D, Tables D1, D2, D3, D4, D5, D6, and D7. With the paired-pulse ISI of 30 ms, the paired-pulse ISI of 70 ms, and the control protocol no significant differences existed. However, with the paired-pulse 10 ms, 50 ms, and 90 ms ISI, as well as with the single pulse significant differences could be seen. With the 10 ms paired-pulse, the significant differences started to occur in the late potentials in trials 41-60 compared with trials 1-20 between 200 and 280 ms, and between 380 and 420 ms. Similar difference occured also in the 50 ms ISI paired-pulse protocol, however, not as strongly as the difference became significant only between 200 and 240 ms.

The differences in the 90 ms ISI paired-pulse and in the single pulse also seemed to follow a common trend. TMS-evoked potentials in the 90 ms ISI paired-pulse began to have significant differences already in trials 21-40 compared with trials 1-20 between 320 and 400 ms. With the single pulse, significant differences also occured already in trials 21-40 compared with trials 1-20 between 360 and 420 ms.

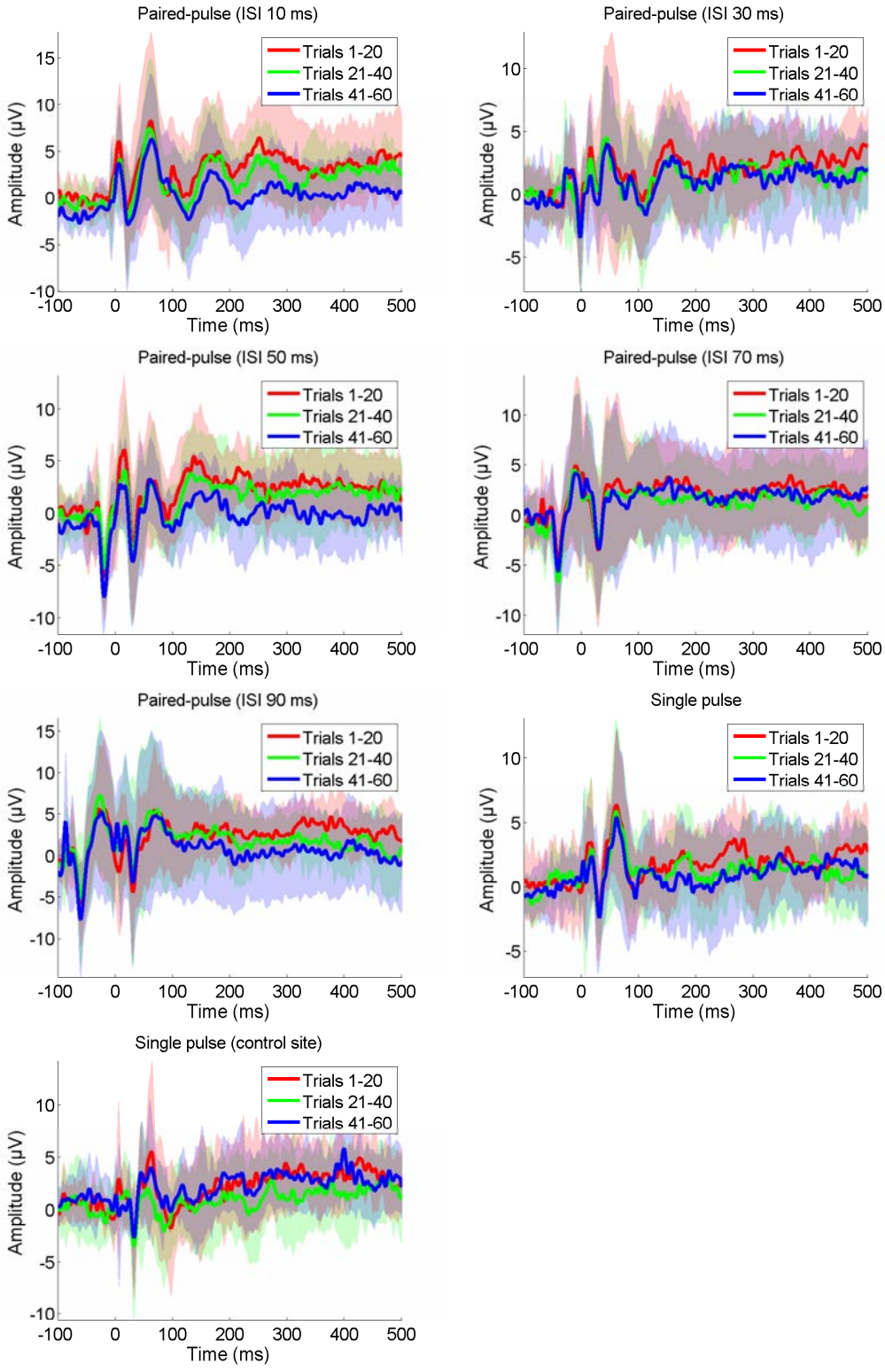

Figure 24: Trials 1-20, trials 21-40, and trials 41-60 plotted for each protocol. The faint curves represent the intersubject variation (± 1 standard deviation).

Trends in the frequency bands over trials are presented in Figure 25. All the frequency bands had quite similar power levels. In addition, in all the protocols, the beta band had the biggest power. Furthermore, with 10 ms, 30ms, and 90 ms ISI paired-pulse protocols there was a large peak in power levels during the first few trials, perhaps due to the movement of the subjects in the beginning of the TMS stimulation.

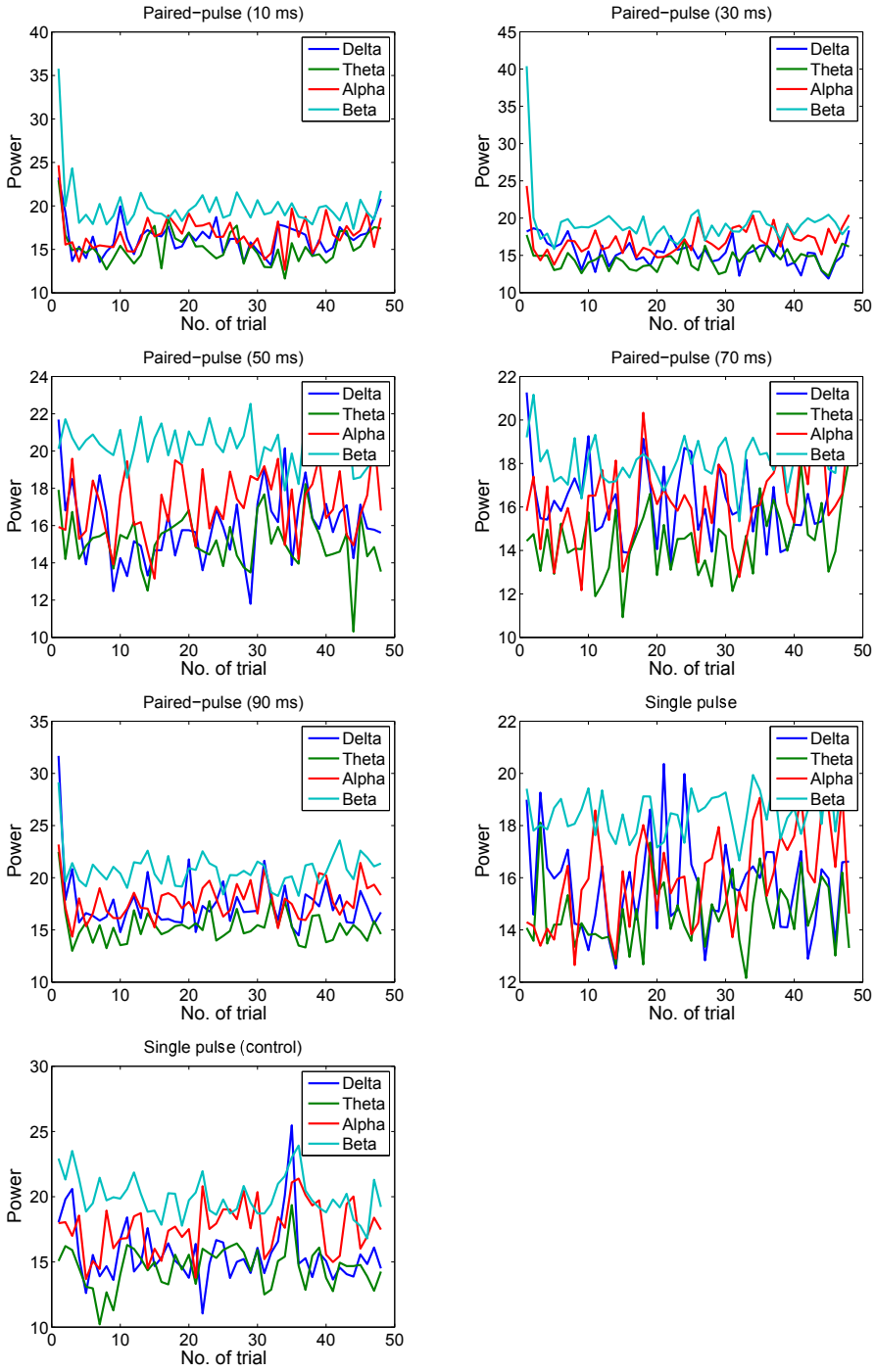

Figure 25: Power in delta, theta, alpha, and beta frequency bands averaged over subjects in each trial. Only 50 first trials are shown.

4.5 Spreading of the TMS-evoked EEG responses

The scalp maps of the TMS-evoked potentials are shown for the paired-pulse protocol with an ISI of 10 ms in Figure 26, for the single pulse in Figure 27, and for the

control protocol in Figure 28. The scalp maps of the other paired-pulse protocols (ISI of 30 ms, 50 ms, 70 ms, 90 ms) can be seen in Appendix E, Figures E1, E2, E3, and E4. The data in all the figures is presented in a way that the zero point in time indicates either the second pulse or the single pulse depending whether a paired-pulse or a single pulse protocol is applied, respectively.

The profile of the TMS-evoked potential of the paired-pulse protocol with an ISI of 10 ms began with centroparietal and posterior positivity from 0 to 40 ms. The greatest activity was not centered under the stimulation spot, but the activity extended to the centroparietal area. Between 40 and 120 ms there was a posterior positivity and frontal negativity. After this, there was positivity in the centroparietal area from 120 ms to 360 ms.

With the single pulse protocol on the primary visual cortex, the profile of the TMS-evoked potential had posterior positivity in the stimulation area between 0 and 20 ms, followed by frontal positivity and posterior negativity from 20 to 40 ms. After this, the posterior area changed to positive from 40 to 120 ms, followed by centroparietal positivity between 140 and 340 ms. In the end between 340 and 480 ms, there was posterior positivity and centrofrontal negativity.

On the control site, the single pulse had a very clustered positive activation right under the stimulation region (near electrode CPz) between 0 and 140 ms. This was followed by centroparietal positivity from 140 to 320 ms, and lastly, there was posterior parietal positivity and centrofrontal negativity between 320 and 460 ms.

With paired-pulse protocols with an ISI of 30 ms, 50 ms, 70 ms, and 90 ms the scalp maps showed individual differences between the protocols, but some common trends were found. These were centroparietal positivity approximately from 100 ms onwards and centroparietal and frontal negativity approximately from 300 ms onwards.

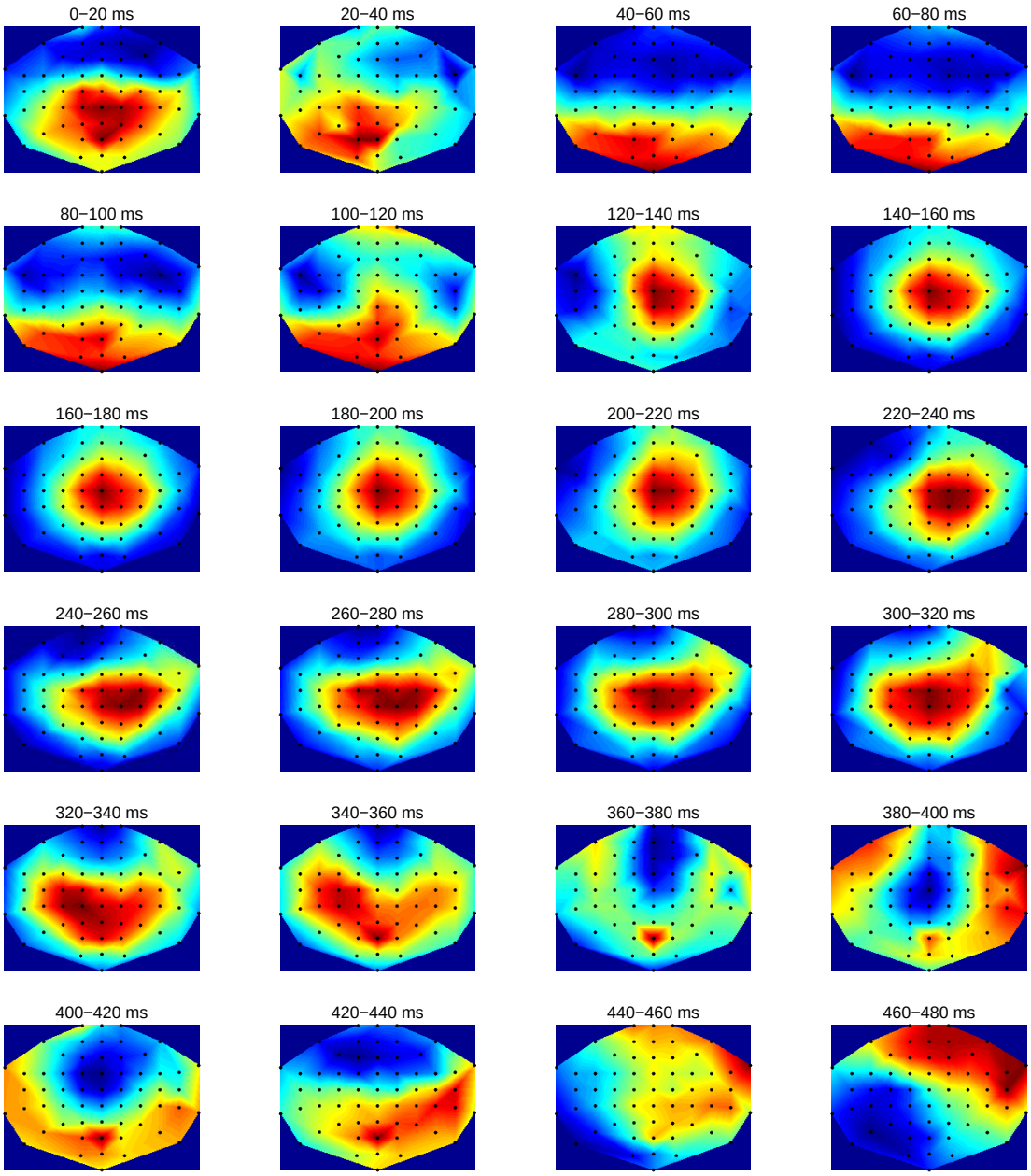

Figure 26: The scalp maps of the paired-pulse protocol (ISI 10 ms) TMS-evoked EEG from the primary visual cortex. The data is presented as the mean amplitude between 20 ms time windows. The data is shifted so that the zero point marks the start of the second pulse. The colour red indicates positive amplitude and blue negative.

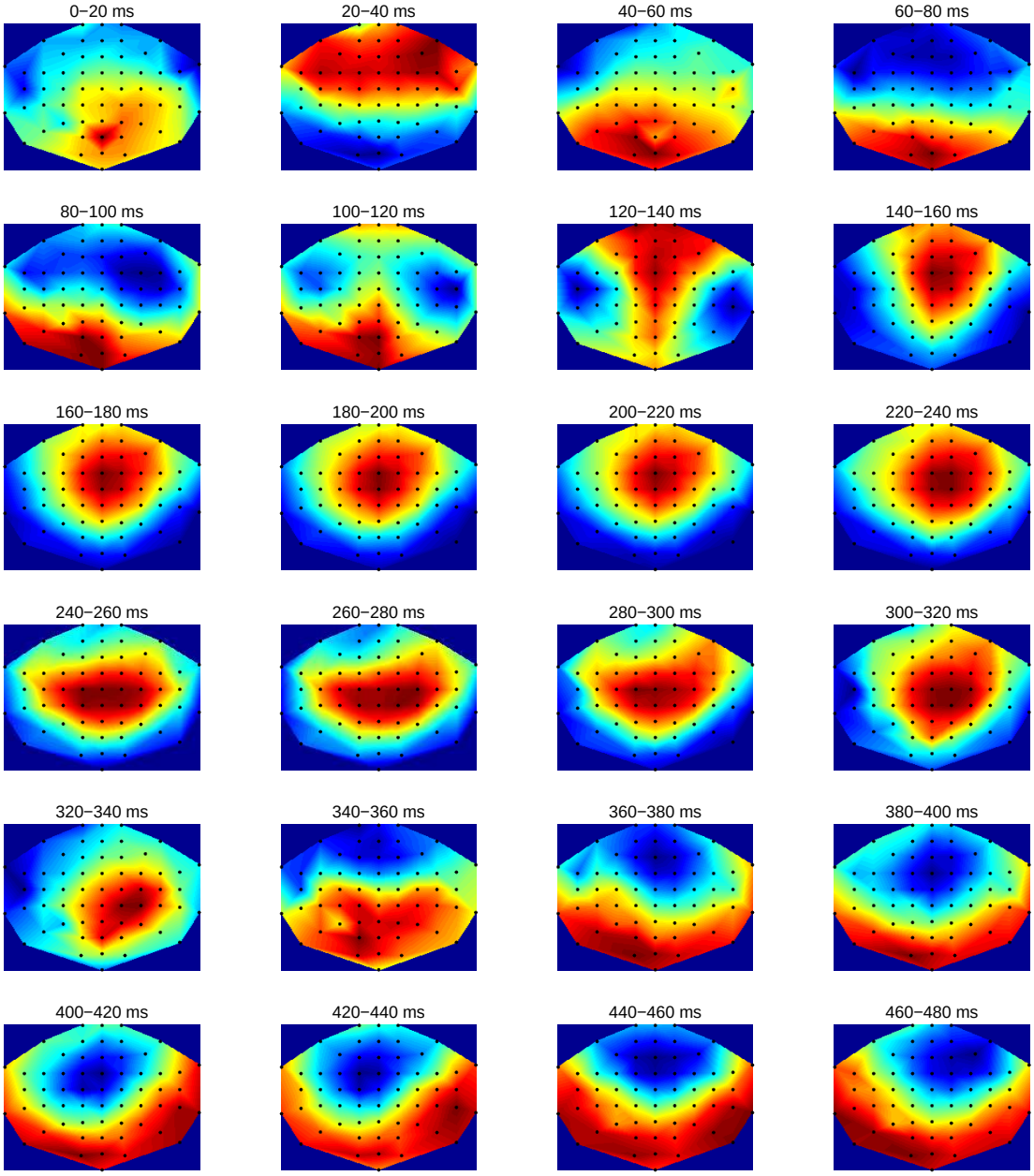

Figure 27: The scalp maps of the single pulse TMS-evoked EEG from the primary visual cortex. The data is presented as the mean amplitude of 20 ms time windows. The data is presented so that the zero point marks the start of the pulse. The colour red indicates positive amplitude and blue negative.

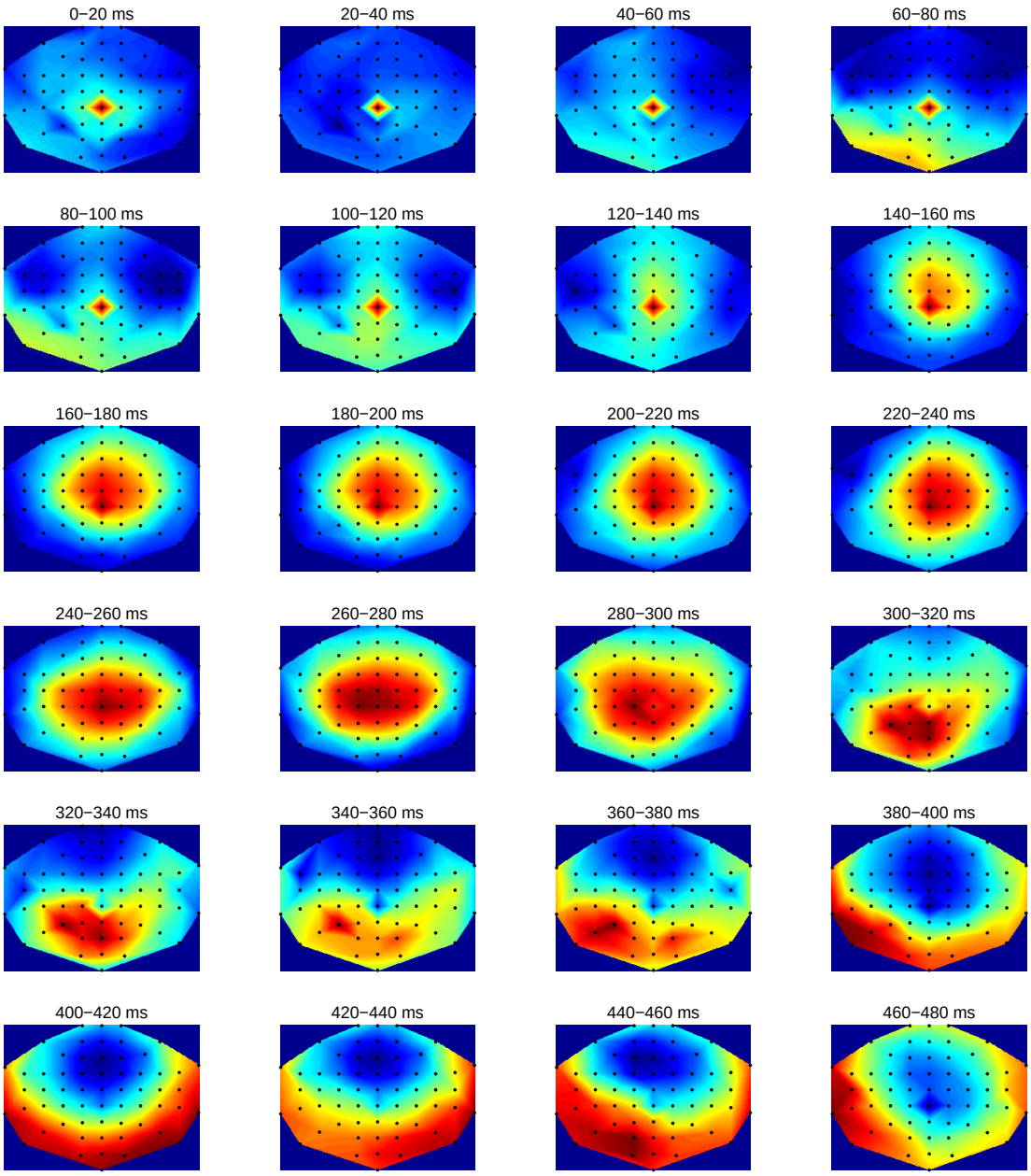

Figure 28: The scalp maps of the single pulse TMS-evoked EEG from the centro-parietal control site (left from electrode CPz). The data is presented as the mean amplitude of 20 ms time windows. The zero point on the time axis is the start of the pulse. The colour red indicates positive amplitude and blue negative.

The results from the two-tailed paired t-test in three different brain areas are presented in Appendix F, Tables F1, F2, and F3. In the right occipital lobe (Figure 29), the potentials were still similar as the only significant difference was with the paired-pulse protocol of 10 ms ISI in the time interval between 400 and 440 ms. In the dorsoprefrontal area (Figure 30), differences started to be greatly significant.

With ISI of 10 ms, significant differences were between 100 and 140 ms, as well as between 400 and 420 ms. With slightly longer ISI of 30 ms, the differences were between 80 and 140 ms, 180 and 220 ms, and 360 and 400 ms. With 50 ms ISI, significant differences were from 0 to 40 ms, 80 to 140 ms, and 300 to 340 ms. With 70 ms ISI significant differences were between 0 and 40 ms, 60 and 140 ms, 160 and 240 ms, and 300 and 340 ms. With the longest ISI of 90 ms, significant differences were in time intervals between 40 and 120 ms, 160 and 320 ms, and 360 and 420 ms. Overall, the longer the ISI, the more the single pulse response differed from the paired-pulse response.

On the motoe cortex (Figure 31), significant differences were found with 10 ms ISI between 400 and 440 ms and with 30 ms ISI between 20 and 80 ms, and 100 and 160 ms. With 50 ms ISI, significant values were between 20 and 60 ms, 80 and 140 ms, and 320 and 360 ms. With ISI of 70 ms, significant differences were between 80 and 120 ms, and between 400 and 440 ms. With the longest ISI of 90 ms, significant differences were between 0 and 40 ms, 60 and 120 ms, 160 and 220 ms, 240 and 300 ms, and between 380 and 440 ms.

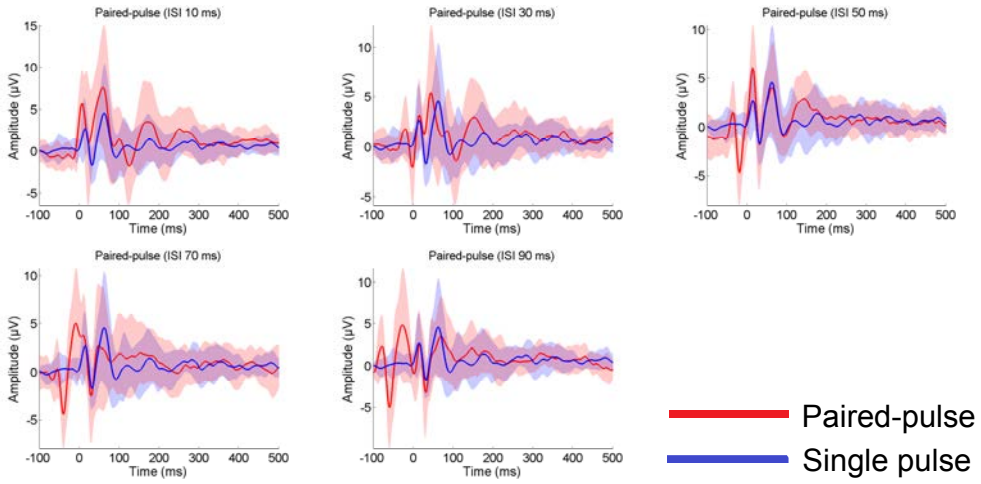

Figure 29: TMS-evoked potentials in the right occipital lobe. The faint curves represent the intersubject variation (± 1 standard deviation).

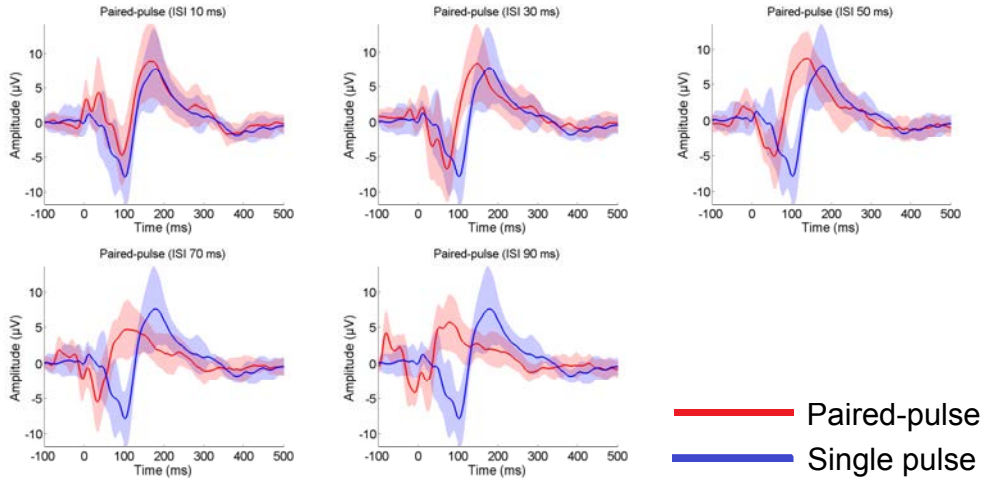

Figure 30: TMS-evoked potentials in the dorsoprefrontal cortex. The faint curves represent the intersubject variation (± 1 standard deviation).

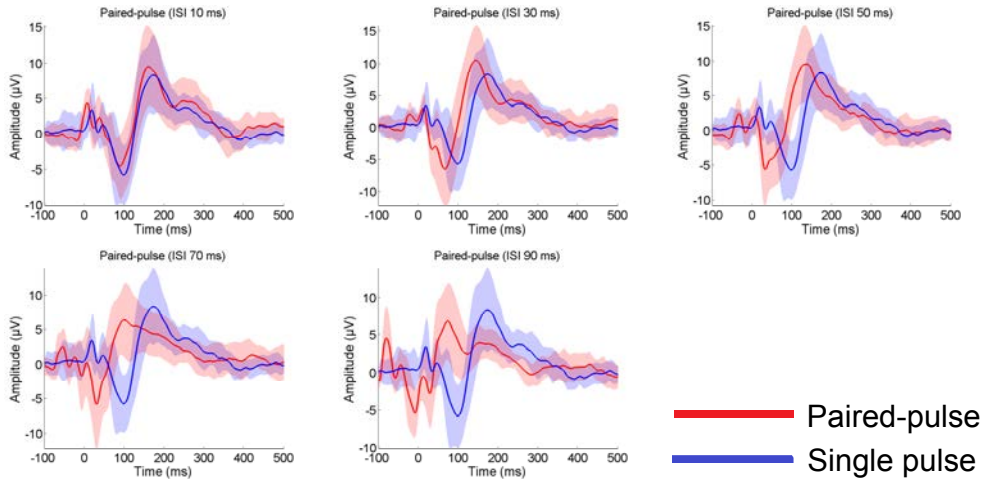

Figure 31: TMS-evoked potentials in the motor cortex. The faint curves represent the intersubject variation (± 1 standard deviation).

4.6 Frequency contents of TMS-evoked potentials

The results from the two-tailed paired t-test are presented in Appendix G, Table G1. The boxplot of the power values in each frequency band is shown in Figure 32. No significant differences were found.

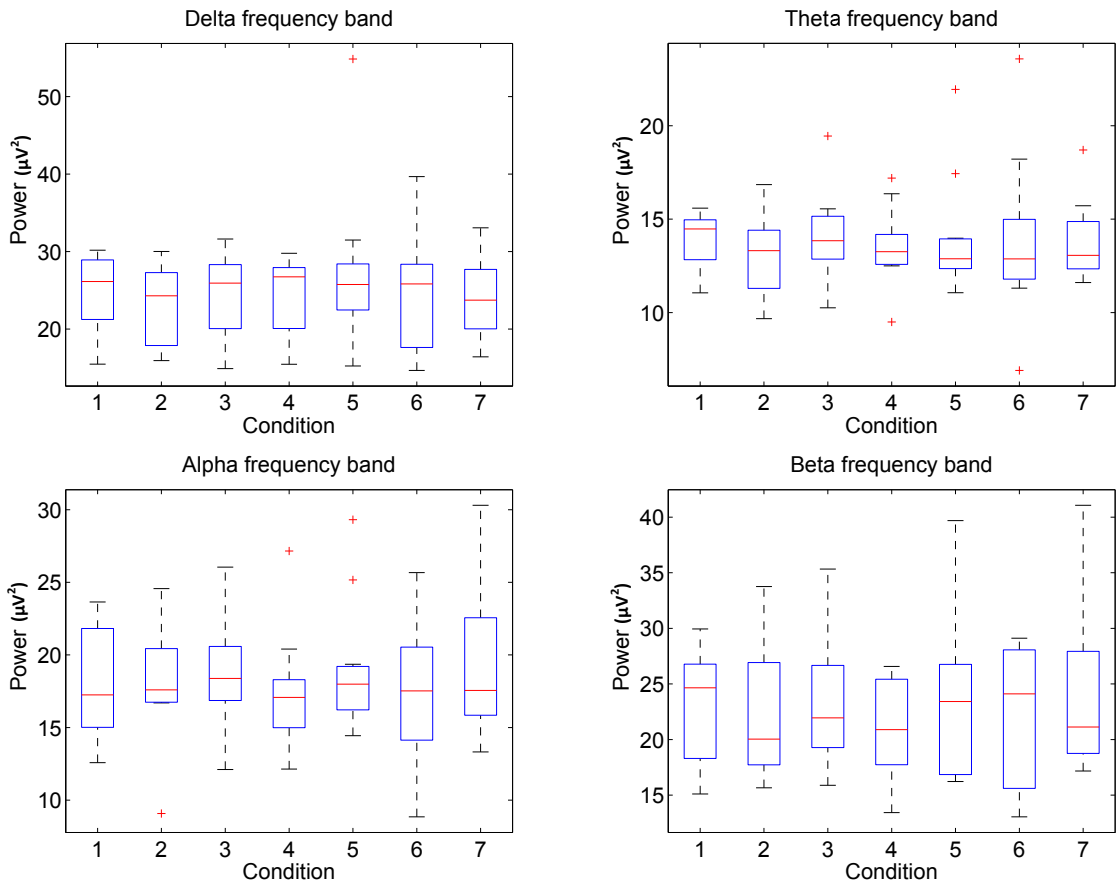

Figure 32: A boxplot of the frequency contents of the TMS-evoked EEG potentials. Conditions are marked as 1=paired-pulse (10 ms), 2=paired-pulse (30 ms), 3=paired-pulse (50 ms), 4=paired-pulse (70 ms), 5=paired-pulse (90 ms), 6=single pulse, 7=single pulse (control site). The red horizontal line shows the median value, the box shows the upper and lower quartile, the whiskers show the extreme values, and the crosses outside the whiskers present the outliers.

5 Discussion and conclusions

5.1 Artefact reduction

The TMS-evoked artefact reduction of the EEG recorded from the primary visual cortex and from the control area on central parietal cortex succeeded relatively well. It was evident that the largest muscle artefacts were removed from the data. In cases where the algorithm failed, the cause may have been in the author who interpreted the data, as the interpretation of ICA results is subjective. However, before more accurate conclusions can be made, some quantitative analysis needs to be done, as the efficiency of ICA was only considered qualitatively. An ICA algorithm which is fully automatic exists and its details can be found from [58]. The exact implementation was not, however, published yet so it was not used in the present study.

5.2 Facilitation and inhibition in the TMS-evoked EEG

In the visual cortex, Moliadze et al. made a study on facilitation and inhibition using an anaesthetized cat as a subject [68]. They tried different combinations of test and conditioning stimulus intensities and found out that the facilitation and inhibition phenomena depend strongly on the strength of the condition stimulus compared with the test stimulus [68]. In the present study, both the test stimulus and conditioning stimulus were given at an equal intensity. One reason why in the current study no traces of facilitation nor inhibition were found might be due to this. Moliadze et al. hypothesized that when the test and conditioning stimulus are identical, the same neuronal population is stimulated, and when they are not identical different neuronal populations are activated [68]. Inhibitory and excitatory neurons respond differently for the same stimulus set due to their different synapses [68]. When the test and conditioning stimulus are identical, there should not be any inhibitory effect, but facilitation is possible [68]. In the present study, significant results indicating either facilitation or inhibition were not found.

5.3 TMS-evoked phosphenes

The exploratory phosphene results from the TMS experiment may have supported the findings from Sparing et al [34]. Sparing observed that ISIs between 2 and 12 ms facilitate phosphene perception [34]. This was inconsistent with the findings on the motor cortex. In the present study, the smallest ISI was 10 ms, which in qualitative analysis may have facilitated phosphenes compared with the single pulse protocol. Another ISI which may have facilitated phosphene perception was 30 ms. Longer ISI of 50, 70 and 90 ms may have induced inhibition.

In previous phosphene related studies approximately half of the subjects reported seeing phosphenes [42] [69] [44]. This was not observed in the present study, as less than half of the subjects perceived phosphenes. Subjects who perceived phosphenes in both the TMS-EEG and the TMS experiment were strongly characterized as being participated in phosphene studies several times previously. It has been found in an fMRI study made by Meister et al. that there are significant differences between primary visual cortex activations and visual-evoked potentials in response to a checkerboard pattern stimuli between subjects who saw phosphenes and who did not [70]. This discovery indicated that intersubject functional differences may affect the individual tendencies in subjects seeing phosphenes [70]. It may be that subjects with previous experience in similar studies happened to have the optimal functional abilities to perceive phosphenes in the present study. In addition, in the TMS-EEG experiment, the electric field in the brain may have not been sufficient enough to produce phosphenes, as the coil could not be placed directly on the scalp but on top of the EEG electrodes. This caused longer distance to neural tissue and so reduced the induced electric field strength in the cortex. In addition, the phosphene threshold was determined when the subjects had their eyes closed, even though in the main experiment they had their eyes open. It may be that the phosphene threshold

during eyes open and eyes closed was different.

To increase the number of subjects perceiving phosphenes, prior to the main experiment different brain area from the phosphene inductive visual cortex, for example the motor cortex, should have been stimulated to provide a comparison for the phosphene perception, as some of the subjects were totally naive to TMS. Also, Silvanto et al. have found that stimulation of areas connected to V1, such as the posterior parietal cortex [71], or frontal eye fields reduce the phosphene threshold [72]. In addition, the black computer screen used in the experiment was reported by a few subjects to have irregular darkness, which may have affected the phosphene perception. Furthermore, the well-known effects of state-dependency were not taken into account in the study, as for example, the fatigue level of subjects and the number of times the subjects had participated in phosphene related TMS studies were not controlled.

With single-pulse TMS [32] and short ISI [34], it has been found that the lowest phosphene threshold can be obtained when the direction of the induced current is from lateral to medial. However, with longer paired-pulse protocols on the visual cortex no similar studies have been made. When making explorative tests before conducting the present study, it was found that it was easier to perceive phosphenes with a biphasic coil. However, paired-pulses could only be given with a monophasic coil.

5.4 Cumulation effects

Julkunen et al. discovered, that by altering the ITI the amplitudes of the motor evoked potentials in the motor cortex vary [73]. In the primary visual cortex the effects of different ITI on EEG are still unknown. In the present study, the ITI value was fixed to 3334 ms. Whether the choice influenced the results, for example the grand averages, cumulation effects were analyzed. It was found that with the paired-pulse protocol with ISI of 10 ms, 50 ms, and 90 ms, as well as with the single pulse protocol there might have been some cumulation. Alternatively, with these stimulation protocols TMS might have triggered neural processes which summated to the evoked potentials.

5.5 Spreading of the TMS-evoked EEG responses

In the scalp maps, the components of centroparietal positivity were present in all of the protocols approximately around the time window between 100 and 280 ms. In addition, in each of the protocols there was some frontocentral negativity right after the TMS pulse. Taylor et al. also found similar phenomena with single pulses on the primary visual cortex and on the same control-site as the one in the present study [30]. Their hypothesis was that these activations reflect sensory-specific auditory and tactile potentials evoked by TMS [30]. In other words, these components were

artefacts. In addition, they hypothesized that the later components approximately after 220 ms are related to the primary visual cortex stimulation and are not found in the control area. With the scalp maps in the present study, this was not evident, as most of the protocols seemed to have similar later components of frontocentral negativity and posterior-parietal positivity.

In the present study, the single pulse activation in the control area, which was left from the electrode CPz, stayed local approximately for 100 ms before the activation reached other brain areas. With stimulation protocols on the primary visual cortex, the activation shifted to other brain areas approximately after 20 ms after the TMS pulse. In a study by Bestmann et al. it was found that TMS either facilitates or inhibits corticocortical functional connectivity, depending on the initial states of these regions [74]. In the present study, the stimulation protocols were applied at random order, so the initial state of the regions should have not explained the difference, and there were some other factors causing the phenomenon, maybe due to anatomy or due to function of the stimulation area. Taking the diffusion tensor images (DTI) of the subjects would have brought more information on the anatomical connectivity and spreading of the TMS-evoked potentials [75].

By analyzing the differences of the TMS-evoked potentials of the paired-pulse protocols compared with the single pulse protocol on the primary visual cortex outside the stimulation location some interesting results were obtained. Near the stimulation spot, on the right occipital lobe, only short-lasting difference occured with the 10 ms protocol. When the distance to the stimulation spot increased, more and longer-lasting differences were found. In addition, outside the stimulation location the longer the ISI of the paired-pulse protocol, the more different the potentials were. These results were obtained from potentials averaged over several electrodes, which might have affected the results, and it would have been better to analyse the potentials also on single electrode level.

5.6 Frequency contents of TMS-evoked potentials

TMS evokes EEG responses, but can also trigger EEG oscillations [76] [77] or disrupt ongoing rhythms [78]. Due to the present experimental design, the oscillations were studied only by comparing the power in the frequency bands between paired-pulse protocols and the single pulse protocol. No significant differences were found. This might have indicated that the applied paired-pulse protocols had the same effects on the EEG as the single pulse or differences could not be obtained due to intersubject variation. However, to get more information on this, more analysis should be done, such as time-frequency analysis.

5.7 Concluding remarks

This master's thesis included an artefact removal and an exploratory cognitive analysis. It seemed that ICA may be an useful method to remove the TMS-evoked

artefacts from EEG data recorded from the primary visual cortex. In the cognitive analysis the responses to the paired-pulse protocols differed from the responses to the single pulse TMS only in spatial spreading. However, as the data analysis revealed several problems in the experimental setup, no final conclusions could be drawn. In addition, as the results of the TMS stimulation studies combined with the measurement of EEG are sensitive to experimental conditions [31], the results received in this study were dependent of the used experimental design.

For a better controlled and stable study, the primary visual cortex of each subject should have been located before the TMS experiment by using fMRI. Also, during the TMS-EEG measurement the stimulation location should have been controlled better as all the subjects were stimulated in slightly different areas and evoked potentials depend greatly on the exact coil location [79]. Lioumis et al. have found that in a controlled measurement, the TMS-evoked averaged EEG potentials are highly reproducible [80]. In addition, more subjects perceiving phosphenes, more trials per condition, and more homogeneous subject group would have been beneficial. With large intersubject variation and few subjects finding statistically significant differences is unlikely.

References

[1] M. Bear, B. Connors, and M. Paradiso, *Neuroscience: Exploring the Brain*. Lippincott Williams & Wilkins, third edit ed., 2007.

[2] S. Jacobson and E. M. Marcus, *Neuroanatomy for the Neuroscientist*. Springer, 2008.

[3] J. Carey, *Brain Facts: A Primer on the Brain and Nervous System*. Washington, DC: Society for Neuroscience, 1990.

[4] C. Salustri, F. Tecchio, F. Zappasodi, G. Bevacqua, M. Fontana, M. Ercolani, D. Milazzo, R. Squitti, and P. M. Rossini, "Cortical excitability and rest activity properties in patients with depression.," *Journal of psychiatry & neuroscience : JPN*, vol. 32, pp. 259–66, July 2007.

[5] H. Mäki, *Doctoral dissertation: Studying the Cortical State with Transcranial Magnetic Stimulation*. Article dissertation, Aalto University, 2011.

[6] A. A. Kühn, P. Grosse, K. Holtz, P. Brown, B.-U. Meyer, and A. Kupsch, "Patterns of abnormal motor cortex excitability in atypical parkinsonian syndromes.," *Clinical neurophysiology : official journal of the International Federation of Clinical Neurophysiology*, vol. 115, pp. 1786–95, Aug. 2004.

[7] F. Gilio, a. Currà, M. Inghilleri, C. Lorenzano, a. Suppa, M. Manfredi, and a. Berardelli, "Abnormalities of motor cortex excitability preceding movement in patients with dystonia.," *Brain : a journal of neurology*, vol. 126, pp. 1745–54, Aug. 2003.

[8] S. Berweck, M. Walther, V. Brodbeck, N. Wagner, I. Koerte, V. Henschel, H. Juenger, M. Staudt, and V. Mall, "Abnormal motor cortex excitability in congenital stroke.," *Pediatric research*, vol. 63, pp. 84–8, Jan. 2008.

[9] K. J. Werhahn, J. Lieber, J. Classen, and S. Noachtar, "Motor cortex excitability in patients with focal epilepsy.," *Epilepsy research*, vol. 41, pp. 179–89, Sept. 2000.

[10] H. Blumenfeld, *Neuroanatomy Through Clinical Cases (Blumenfeld,Neuroanatomy through Clinical Cases)*. Sinauer Associates, 2002.

[11] Canadian Institutes of Health Research, "The Brain from Top to Bottom." `http://thebrain.mcgill.ca/flash/a/a_02/a_02_cr/a_02_cr_vis/a_02_cr_vis.html`, 2012. [Read on 8.6.2012.].

[12] T. Wagner, A. Valero-Cabre, and A. Pascual-Leone, "Noninvasive human brain stimulation.," *Annual review of biomedical engineering*, vol. 9, pp. 527–65, Jan. 2007.

[13] P. M. Rossini and S. Rossi, "Transcranial magnetic stimulation: diagnostic, therapeutic, and research potential.," *Neurology*, vol. 68, pp. 484–8, Mar. 2007.

[14] J. O'Shea and V. Walsh, "Transcranial magnetic stimulation.," *Current biology : CB*, vol. 17, pp. R196–9, Mar. 2007.

[15] M. Hallett, "Transcranial magnetic stimulation and the human brain.," *Nature*, vol. 406, pp. 147–50, July 2000.

[16] R. J. Ilmoniemi, J. Ruohonen, and J. Karhu, "Transcranial magnetic stimulation–a new tool for functional imaging of the brain.," *Critical reviews in biomedical engineering*, vol. 27, pp. 241–84, Jan. 1999.

[17] R. Bartholow, "Experimental investigation into the functions of the human brain," *American Journal of the Medical Sciences*, vol. 66, no. 134, pp. 305–313, 1874.

[18] T. Wagner, J. Rushmore, U. Eden, and A. Valero-Cabre, "Biophysical foundations underlying TMS: setting the stage for an effective use of neurostimulation in the cognitive neurosciences.," *Cortex; a journal devoted to the study of the nervous system and behavior*, vol. 45, pp. 1025–34, Oct. 2009.

[19] R. J. Ilmoniemi, J. Ruohonen, and J. Karhu, "Transcranial magnetic stimulation–a new tool for functional imaging of the brain.," *Critical reviews in biomedical engineering*, vol. 27, pp. 241–84, Jan. 1999.

[20] E. M. Wassermann, C. M. Epstein, U. Ziemann, V. Walsh, T. Paus, and S. H. Lisanby, *The Oxford Handbook of Transcranial Stimulation*. Oxford University Press, 2008.

[21] C. D and C. BN, "Developing a more focal magnetic stimulator. Part I: Some basic principles.," Jan. 1991.

[22] T. Paus, R. Jech, C. J. Thompson, R. Comeau, T. Peters, and a. C. Evans, "Transcranial magnetic stimulation during positron emission tomography: a new method for studying connectivity of the human cerebral cortex.," *The Journal of neuroscience : the official journal of the Society for Neuroscience*, vol. 17, pp. 3178–84, May 1997.

[23] R. J. Ilmoniemi and D. Kičić, "Methodology for combined TMS and EEG.," *Brain topography*, vol. 22, pp. 233–48, Jan. 2010.

[24] R. J. Ilmoniemi, J. Virtanen, J. Ruohonen, J. Karhu, H. J. Aronen, R. Näätänen, and T. Katila, "Neuronal responses to magnetic stimulation reveal cortical reactivity and connectivity.," *Neuroreport*, vol. 8, pp. 3537–40, Nov. 1997.

[25] S. Nagarajan and D. Durand, "Effects of induced electric fields on finite neuronal structures: a simulation study," *, IEEE Transactions on*, vol. 40, no. 92, 1993.

[26] J. Silvanto, N. G. Muggleton, A. Cowey, and V. Walsh, "Neural adaptation reveals state-dependent effects of transcranial magnetic stimulation.," *The European journal of neuroscience*, vol. 25, pp. 1874–81, Mar. 2007.

[27] M. Carandini and D. Ferster, "A tonic hyperpolarization underlying contrast adaptation in cat visual cortex.," *Science (New York, N.Y.)*, vol. 276, pp. 949–52, May 1997.

[28] N. Arai, S. Okabe, T. Furubayashi, Y. Terao, K. Yuasa, and Y. Ugawa, "Comparison between short train, monophasic and biphasic repetitive transcranial magnetic stimulation (rTMS) of the human motor cortex.," *Clinical neurophysiology : official journal of the International Federation of Clinical Neurophysiology*, vol. 116, pp. 605–13, Mar. 2005.

[29] M. Sommer, A. Alfaro, M. Rummel, S. Speck, N. Lang, T. Tings, and W. Paulus, "Half sine, monophasic and biphasic transcranial magnetic stimulation of the human motor cortex.," *Clinical neurophysiology : official journal of the International Federation of Clinical Neurophysiology*, vol. 117, pp. 838–44, Apr. 2006.

[30] P. Taylor and V. Walsh, "The neural signature of phosphene perception," *Human brain mapping*, vol. 31, no. 9, pp. 1408–1417, 2010.

[31] J. Silvanto, N. Muggleton, and V. Walsh, "State-dependency in brain stimulation studies of perception and cognition.," *Trends in cognitive sciences*, vol. 12, pp. 447–54, Dec. 2008.

[32] T. Kammer, S. Beck, M. Erb, and W. Grodd, "The influence of current direction on phosphene thresholds evoked by transcranial magnetic stimulation.," *Clinical neurophysiology : official journal of the International Federation of Clinical Neurophysiology*, vol. 112, pp. 2015–21, Nov. 2001.

[33] T. Kujirai, M. Caramia, and J. Rothwell, "Corticocortical inhibition in human motor cortex.," *The Journal of Physiology*, pp. 501–519, 1993.

[34] R. Sparing, N. Dambeck, K. Stock, I. G. Meister, D. Huetter, and B. Boroojerdi, "Investigation of the primary visual cortex using short-interval paired-pulse transcranial magnetic stimulation (TMS).," *Neuroscience letters*, vol. 382, pp. 312–6, July 2005.

[35] M. Inghilleri, A. Berardelli, G. Cruccu, and M. Manfredi, "Silent period evoked by transcranial stimulation of the human cortex and cervicomedullary junction," *Journal of Physiology*, vol. 466, pp. 521–534, 1993.

[36] A. Berardelli, S. Rona, M. Inghilleri, M. Manfredi, S. Neurologiche, R. La, and V. Universita, "Cortical inhibition in Parkinson ' s disease A study with paired magnetic stimulation," *Brain*, pp. 71–77, 1996.

[37] A. Pascual-Leone, N. Davey, J. Rothwell, E. M. Wassermann, and B. K. Puri, *Handbook of Transcranial Magnetic Stimulation*. Hodder Arnold Publishers, 2002.

[38] M. C. Ridding, J. L. Taylor, and J. C. Rothwell, "The effect of voluntary contraction on cortico-cortical inhibition in human motor cortex.," *The Journal of physiology*, vol. 487 (Pt 2, pp. 541–8, Sept. 1995.

[39] U. Ziemann, S. Lönnecker, B. Steinhoff, and W. Paulus, "The effect of lorazepam on the motor cortical excitability in man," *Experimental Brain Research*, vol. 109, Apr. 1996.

[40] M. Oliveri, C. Caltagirone, M. M. Filippi, R. Traversa, P. Cicinelli, P. Pasqualetti, and P. M. Rossini, "Paired transcranial magnetic stimulation protocols reveal a pattern of inhibition and facilitation in the human parietal cortex.," *The Journal of physiology*, vol. 529 Pt 2, pp. 461–8, Dec. 2000.

[41] M. Oliveri, P. M. Rossini, M. M. Filippi, R. Traversa, P. Cicinelli, M. G. Palmieri, P. Pasqualetti, and C. Caltagirone, "Time-dependent activation of parieto-frontal networks for directing attention to tactile space. A study with paired transcranial magnetic stimulation pulses in right-brain-damaged patients with extinction.," *Brain : a journal of neurology*, vol. 123 (Pt 9, pp. 1939–47, Sept. 2000.

[42] B. Boroojerdi, K. O. Bushara, B. Corwell, I. Immisch, F. Battaglia, W. Muellbacher, and L. G. Cohen, "Enhanced excitability of the human visual cortex induced by short-term light deprivation.," *Cerebral cortex (New York, N.Y. : 1991)*, vol. 10, pp. 529–34, May 2000.

[43] B. Boroojerdi, A. Prager, W. Muellbacher, and L. G. Cohen, "Reduction of human visual cortex excitability using 1-Hz transcranial magnetic stimulation," *Neurology*, vol. 54, pp. 1529–1531, Apr. 2000.

[44] R. Sparing, F. M. Mottaghy, G. Ganis, W. L. Thompson, R. Töpper, S. M. Kosslyn, and A. Pascual-Leone, "Visual cortex excitability increases during visual mental imagery–a TMS study in healthy human subjects.," *Brain research*, vol. 938, pp. 92–7, May 2002.

[45] B. Boroojerdi, I. G. Meister, H. Foltys, R. Sparing, L. G. Cohen, and R. Töpper, "Visual and motor cortex excitability: a transcranial magnetic stimulation study.," *Clinical neurophysiology : official journal of the International Federation of Clinical Neurophysiology*, vol. 113, pp. 1501–4, Sept. 2002.

[46] a. Fumal, V. Bohotin, M. Vandenheede, L. Seidel, a. Maertens de Noordhout, and J. Schoenen, "Motor and phosphene thresholds to transcranial magnetic stimuli: a reproducibility study.," *Acta neurologica Belgica*, vol. 102, pp. 171–5, Dec. 2002.

[47] V. Moliadze, Y. Zhao, U. Eysel, and K. Funke, "Effect of transcranial magnetic stimulation on single-unit activity in the cat primary visual cortex.," *The Journal of physiology*, vol. 553, pp. 665–79, Dec. 2003.

[48] V. Romei, V. Brodbeck, C. Michel, A. Amedi, A. Pascual-Leone, and G. Thut, "Spontaneous fluctuations in posterior alpha-band EEG activity reflect variability in excitability of human visual areas.," *Cerebral cortex (New York, N.Y. : 1991)*, vol. 18, pp. 2010–8, Sept. 2008.

[49] V. Jurcak, D. Tsuzuki, and I. Dan, "10/20, 10/10, and 10/5 Systems Revisited: Their Validity As Relative Head-Surface-Based Positioning Systems.," *NeuroImage*, vol. 34, pp. 1600–11, Feb. 2007.

[50] R. a. Tyrrell and D. A. Owens, "A rapid technique to assess the resting states of the eyes and other threshold phenomena: The Modified Binary Search (MOBS)," *Behavior Research Methods, Instruments, & Computers*, vol. 20, pp. 137–141, Mar. 1988.

[51] H. Jasper, "The ten-twenty electrode system of the International Federation. Electroencephalography," *Clinical Neurophysiology*, vol. 10, pp. 370–375, 1958.

[52] U. Herwig, P. Satrapi, and C. Schönfeldt-Lecuona, "Using the international 10-20 EEG system for positioning of transcranial magnetic stimulation.," *Brain topography*, vol. 16, pp. 95–9, Jan. 2003.

[53] J. Virtanen, J. Ruohonen, R. Näätänen, and R. J. Ilmoniemi, "Instrumentation for the measurement of electric brain responses to transcranial magnetic stimulation.," *Medical & biological engineering & computing*, vol. 37, pp. 322–6, May 1999.

[54] R. Oostenveld, P. Fries, E. Maris, and J.-M. Schoffelen, "FieldTrip: Open source software for advanced analysis of MEG, EEG, and invasive electrophysiological data.," *Computational intelligence and neuroscience*, vol. 2011, p. 156869, Jan. 2011.

[55] R. Vigário, J. Särelä, V. Jousmäki, M. Hämäläinen, and E. Oja, "Independent component approach to the analysis of EEG and MEG recordings.," *IEEE transactions on bio-medical engineering*, vol. 47, pp. 589–93, May 2000.

[56] M. Hamidi, H. a. Slagter, G. Tononi, and B. R. Postle, "Brain responses evoked by high-frequency repetitive transcranial magnetic stimulation: an event-related potential study.," *Brain stimulation*, vol. 3, pp. 2–14, Jan. 2010.

[57] M. Iwahashi, T. Arimatsu, S. Ueno, and K. Iramina, "Differences in evoked EEG by transcranial magnetic stimulation at various stimulus points on the head.," *Conference proceedings : ... Annual International Conference of the IEEE Engineering in Medicine and Biology Society. IEEE Engineering in Medicine and Biology Society. Conference*, vol. 2008, pp. 2570–3, Jan. 2008.

[58] R. J. Korhonen, J. C. Hernandez-Pavon, J. Metsomaa, H. Mäki, R. J. Ilmoniemi, and J. Sarvas, "Removal of large muscle artifacts from transcranial magnetic stimulation-evoked EEG by independent component analysis.," *Medical & biological engineering & computing*, vol. 49, pp. 397–407, Apr. 2011.

[59] T. P. Jung, S. Makeig, C. Humphries, T. W. Lee, M. J. McKeown, V. Iragui, and T. J. Sejnowski, "Removing electroencephalographic artifacts by blind source separation.," *Psychophysiology*, vol. 37, pp. 163–78, Mar. 2000.

[60] J. Onton, M. Westerfield, J. Townsend, and S. Makeig, "Imaging human EEG dynamics using independent component analysis.," *Neuroscience and biobehavioral reviews*, vol. 30, pp. 808–22, Jan. 2006.

[61] R. N. Vigário, "Extraction of ocular artefacts from EEG using independent component analysis.," *Electroencephalography and clinical neurophysiology*, vol. 103, pp. 395–404, Sept. 1997.

[62] a. Hyvärinen and E. Oja, "Independent component analysis: algorithms and applications.," *Neural networks : the official journal of the International Neural Network Society*, vol. 13, no. 4-5, pp. 411–30, 2000.

[63] A. Hyvärinen, J. Karhunen, and E. Oja, *Independent Component Analysis (Adaptive and Learning Systems for Signal Processing, Communications and Control Series)*. Wiley-Blackwell, 2001.

[64] T. W. Picton, S. Bentin, P. Berg, E. Donchin, S. a. Hillyard, R. Johnson, G. a. Miller, W. Ritter, D. S. Ruchkin, M. D. Rugg, and M. J. Taylor, "Guidelines for using human event-related potentials to study cognition: recording standards and publication criteria.," *Psychophysiology*, vol. 37, pp. 127–52, Mar. 2000.

[65] S. Komssi, S. Kähkönen, and R. J. Ilmoniemi, "The effect of stimulus intensity on brain responses evoked by transcranial magnetic stimulation.," *Human brain mapping*, vol. 21, pp. 154–64, Mar. 2004.

[66] J. McDonald, *Handbook of Biological Statistics*. Sparky House Publishing, Baltimore, Maryland, 2nd. ed. ed., 2009.

[67] S. Sanei and J. A. Chambers, *EEG Signal Processing*. Wiley-Interscience, 2007.

[68] V. Moliadze, D. Giannikopoulos, U. T. Eysel, and K. Funke, "Paired pulse transcranial magnetic stimulation protocol applied to visual cortex of anaesthetized cat: effects on visually evoked single-unit activity," *The Journal of Physiology*, vol. 3, pp. 955–965, 2005.

[69] B. U. Meyer, R. Diehl, H. Steinmetz, T. C. Britton, and R. Benecke, "Magnetic stimuli applied over motor and visual cortex: influence of coil position and field polarity on motor responses, phosphenes, and eye movements.," *Electroencephalography and clinical neurophysiology. Supplement*, vol. 43, pp. 121–34, Jan. 1991.

[70] I. G. Meister, J. Weidemann, N. Dambeck, H. Foltys, R. Sparing, T. Krings, A. Thron, and B. Boroojerdi, "Neural correlates of phosphene perception.," *Supplements to Clinical neurophysiology*, vol. 56, pp. 305–11, Jan. 2003.

[71] J. Silvanto, N. Muggleton, N. Lavie, and V. Walsh, "The perceptual and functional consequences of parietal top-down modulation on the visual cortex.," *Cerebral cortex (New York, N.Y. : 1991)*, vol. 19, pp. 327–30, Feb. 2009.

[72] J. Silvanto, N. Lavie, and V. Walsh, "Stimulation of the human frontal eye fields modulates sensitivity of extrastriate visual cortex.," *Journal of neurophysiology*, vol. 96, pp. 941–5, Aug. 2006.

[73] P. Julkunen, L. Säisänen, T. Hukkanen, N. Danner, and M. Könönen, "Does second-scale intertrial interval affect motor evoked potentials induced by single-pulse transcranial magnetic stimulation?," *Brain stimulation*, Aug. 2011.

[74] S. Bestmann, O. Swayne, F. Blankenburg, C. C. Ruff, P. Haggard, N. Weiskopf, O. Josephs, J. Driver, J. C. Rothwell, and N. S. Ward, "Dorsal premotor cortex exerts state-dependent causal influences on activity in contralateral primary motor and dorsal premotor cortex.," *Cerebral cortex (New York, N.Y. : 1991)*, vol. 18, pp. 1281–91, June 2008.

[75] D. Le Bihan, J. F. Mangin, C. Poupon, C. a. Clark, S. Pappata, N. Molko, and H. Chabriat, "Diffusion tensor imaging: concepts and applications.," *Journal of magnetic resonance imaging : JMRI*, vol. 13, pp. 534–46, Apr. 2001.

[76] T. Paus, P. K. Sipila, and A. P. Strafella, "Synchronization of Neuronal Activity in the Human Primary Motor Cortex by Transcranial Magnetic Stimulation : An EEG Study Synchronization of Neuronal Activity in the Human Primary Motor Cortex by Transcranial Magnetic Stimulation : An EEG Study," pp. 1983–1990, 2012.

[77] G. Fuggetta, A. Fiaschi, and P. Manganotti, "Modulation of cortical oscillatory activities induced by varying single-pulse transcranial magnetic stimulation intensity over the left primary motor area: a combined EEG and TMS study.," *NeuroImage*, vol. 27, pp. 896–908, Oct. 2005.

[78] M. Rosanova, A. Casali, V. Bellina, F. Resta, M. Mariotti, and M. Massimini, "Natural frequencies of human corticothalamic circuits.," *The Journal of neuroscience : the official journal of the Society for Neuroscience*, vol. 29, pp. 7679–85, June 2009.

[79] S. Komssi, H. J. Aronen, J. Huttunen, M. Kesäniemi, L. Soinne, V. V. Nikouline, M. Ollikainen, R. O. Roine, J. Karhu, S. Savolainen, and R. J. Ilmoniemi, "Ipsi- and contralateral EEG reactions to transcranial magnetic stimulation.," *Clinical neurophysiology : official journal of the International Federation of Clinical Neurophysiology*, vol. 113, pp. 175–84, Feb. 2002.

[80] P. Lioumis, D. Kicić, P. Savolainen, J. P. Mäkelä, and S. Kähkönen, "Reproducibility of TMS-Evoked EEG responses.," *Human brain mapping*, vol. 30, pp. 1387–96, Apr. 2009.

A Technical details of the TMS equipment

Table A1: Technical features of the TMS equipment.

Stimulator		
	Dimensions	Height 98 cm, Width 72 cm, Depth 68 cm
	Weight	140 kg
	Accuracy in intensity variation	+/- 1 % in repeated stimulation
	Accuracy in pulse timing	<0.1 ms
Monophasic coil		
	Mean winding diameter	59 mm
	Outer winding diameter	70 mm
	Monophasic pulse shape	70 μs rising edge, 1 ms total pulse lenght
	Maximum electric field strenght	164 V/m
	Focal area of the stimulation hot spot	0.65 cm^2

B Results from the two-tailed paired t-test to study facilation and inhibition

Table B1: Results from the two-tailed paired t-test on the primary visual cortex. The paired-pulse protocols are compared with single pulse protocol. Only significant results are shown.

	Time window		
Paired-pulse protocol	60-80 ms	140-160 ms	200-220 ms
10 ms	-	-	-
30 ms	p=0.0055	p=0.047	-
50 ms	-	-	-
70 ms	-	-	p=0.049
90 ms	-	-	-

C Results from the repeated measures ANOVA to study facilitation and inhibition

Table C1: Results from the repeated measures ANOVA, paired-pulse (ISI 10ms) compared with single pulse.

Time-window	F-value	p-value
0-20 ms	3.18	0.105
20-40 ms	0.96	0.3493
40-60 ms	1.43	0.2597
60-80 ms	0.82	0.3851
80-100 ms	0.58	0.4656
100-120 ms	0.53	0.4821
120-140 ms	0.3	0.7224
140-160 ms	2.36	0.1554
160-180 ms	1.8	0.2089
180-200 ms	1.68	0.2245
200-220 ms	1.29	0.2826
220-240 ms	3.16	0.1056
240-260 ms	4.57	0.0582
260-280 ms	0.8	0.3912
280-300 ms	4.03	0.0726
300-320 ms	7.2	0.023
320-340 ms	1.28	0.2838
340-360 ms	0.47	0.5088
360-380 ms	0.06	0.8137
380-400 ms	1.96	0.1919
400-420 ms	9.5	0.0116
420-440 ms	2.37	0.1551
440-460 ms	0.31	0.5919
460-480 ms	1.94	0.1937

Table C2: Results from the repeated measures ANOVA, paired-pulse (ISI 30ms) compared with single pulse.

Time-window	F-value	p-value
0-20 ms	0	0.992
20-40 ms	1.54	0.2424
40-60 ms	0.01	0.942
60-80 ms	8.4	0.0159
80-100 ms	0.64	0.4406
100-120 ms	0.17	0.6894
120-140 ms	0.43	0.5268
140-160 ms	3.41	0.0944
160-180 ms	0.31	0.5928
180-200 ms	0.01	0.9208
200-220 ms	0.08	0.7874
220-240 ms	0.96	0.3503
240-260 ms	0.18	0.6809
260-280 ms	0.91	0.3625
280-300 ms	0	0.9925
300-320 ms	0.37	0.5572
320-340 ms	2.68	0.1324
340-360 ms	0.85	0.3774
360-380 ms	2.23	0.1663
380-400 ms	2.69	0.132
400-420 ms	2.17	0.1715
420-440 ms	1.98	0.19
440-460 ms	0.15	0.711
460-480 ms	0.16	0.6966

Table C3: Results from the repeated measures ANOVA, paired-pulse (ISI 50ms) compared with single pulse.

Time-window	F-value	p-value
0-20 ms	1.14	0.31
20-40 ms	0.07	0.7921
40-60 ms	3.04	0.112
60-80 ms	3.19	0.1044
80-100 ms	0	0.9887
100-120 ms	1.31	0.2789
120-140 ms	9.98	0.0102
140-160 ms	2.8	0.1254
160-180 ms	0.63	0.4472
180-200 ms	0.94	0.3559
200-220 ms	9.64	0.011
220-240 ms	3.48	0.0915
240-260 ms	0.07	0.7955
260-280 ms	2.3	0.1602
280-300 ms	0.15	0.7026
300-320 ms	2.35	0.1564
320-340 ms	2.63	0.136
340-360 ms	1.32	0.2771
360-380 ms	0.43	0.5246
380-400 ms	6.44	0.0294
400-420 ms	3.95	0.0749
420-440 ms	2.04	0.1836
440-460 ms	0.52	0.4872
460-480 ms	0.27	0.6145

Table C4: Results from the repeated measures ANOVA, paired-pulse (ISI 70ms) compared with single pulse.

Time-window	F-value	p-value
0-20 ms	0.2	0.6606
20-40 ms	0.26	0.6233
40-60 ms	0.12	0.7372
60-80 ms	0.49	0.4993
80-100 ms	2.71	0.1309
100-120 ms	3.07	0.1101
120-140 ms	1.34	0.2731
140-160 ms	1.65	0.2273
160-180 ms	0.98	0.3466
180-200 ms	2.6	0.1381
200-220 ms	2.97	0.1154
220-240 ms	0.02	0.8846
240-260 ms	0.58	0.4638
260-280 ms	0.75	0.4073
280-300 ms	0.07	0.7909
300-320 ms	4.68	0.0557
320-340 ms	2.3	0.1604
340-360 ms	2.24	0.1657
360-380 ms	2.44	0.1492
380-400 ms	1.55	0.2418
400-420 ms	2.72	0.1298
420-440 ms	3.57	0.088
440-460 ms	0	0.9621
460-480 ms	0.71	0.4192

Table C5: Results from the repeated measures ANOVA, paired-pulse (ISI 90ms) compared with single pulse.

Time-window	F-value	p-value
0-20 ms	1.39	0.2651
20-40 ms	1.2	0.2992
40-60 ms	2.14	0.1746
60-80 ms	0	0.9756
80-100 ms	2.64	0.135
100-120 ms	0.13	0.7287
120-140 ms	0.2	0.664
140-160 ms	0.85	0.3784
160-180 ms	0.01	0.9426
180-200 ms	0.64	0.4424
200-220 ms	0.54	0.4807
220-240 ms	0.07	0.7973
240-260 ms	0.32	0.5868
260-280 ms	1.35	0.2717
280-300 ms	0.01	0.936
300-320 ms	2.75	0.1303
320-340 ms	6.36	0.0303
340-360 ms	2.87	0.1211
360-380 ms	1.87	0.2017
380-400 ms	2.52	0.1435
400-420 ms	2.4	0.1521
420-440 ms	2.9	0.1195
440-460 ms	1.16	0.3058
460-480 ms	0.01	0.9058

D Cumulation effects

Table D1: p-values from the two-tailed paired t-test to study cumulation effects. Paired-pulse condition (ISI 10 ms). Trials 1-20 were compared with trials 21-40, trials 1-20 were compared with trials 41-60, and trials 21-40 were compared with trials 41-60. Avgs1==trials 1-20, avgs2==trials 21-40, avgs3==trials 41-60.

Time-window	avgs1 vs avgs2	avgs1 vs avgs3	avgs2 vs avgs3
0-20	0.1086	0.3278	0.6093
20-40	0.1445	0.0124	0.8029
40-60	0.8300	0.5478	0.6775
60-80	0.9392	0.6009	0.5016
80-100	0.9996	0.0505	0.0066
100-120	0.4615	0.6412	0.4454
120-140	0.3628	0.3404	0.9645
140-160	0.7385	0.2032	0.3353
160-180	0.6637	0.8679	0.5925
180-200	0.9657	0.2113	0.2898
200-220	0.1177	0.0015	0.1814
220-240	0.0114	0.0009	0.0175
240-260	0.1826	0.0011	0.0023
260-280	0.5822	0.0928	0.2198
280-300	0.0595	0.1130	0.9463
300-320	0.0427	0.1338	0.2890
320-340	0.4629	0.2759	0.8991
340-360	0.2031	0.7503	0.0996
360-380	0.9514	0.2617	0.3373
380-400	0.3703	0.0978	0.0423
400-420	0.4292	0.3322	0.0970
420-440	0.2986	0.8807	0.5410
440-460	0.7753	0.1521	0.1650
460-480	0.8163	0.0063	0.0177

Table D2: p-values from the two-tailed paired t-test to study cumulation effects. Paired-pulse condition (ISI 30 ms). Trials 1-20 were compared with trials 21-40, trials 1-20 were compared with trials 41-60, and trials 21-40 were compared with trials 41-60. Avgs1==trials 1-20, avgs2==trials 21-40, avgs3==trials 41-60.

Time-window	avgs1 vs avgs2	avgs1 vs avgs3	avgs2 vs avgs3
0-20	0.4616	0.3129	0.4532
20-40	0.6399	0.7348	0.1139
40-60	0.8231	0.9309	0.6869
60-80	0.5231	0.8376	0.8107
80-100	0.7898	0.9725	0.7768
100-120	0.7515	0.6419	0.8510
120-140	0.7505	0.4442	0.7155
140-160	0.2564	0.3376	0.8442
160-180	0.6104	0.9954	0.5452
180-200	0.6628	0.9378	0.7186
200-220	0.6145	0.8941	0.5243
220-240	0.2147	0.2574	0.8914
240-260	0.8632	0.4471	0.6509
260-280	0.5954	0.0913	0.2960
280-300	0.3590	0.5201	0.5676
300-320	0.4460	0.7330	0.5933
320-340	0.4216	0.2877	0.7927
340-360	0.9585	0.4903	0.4724
360-380	0.8579	0.4529	0.5280
380-400	0.8352	0.235	0.9476
400-420	0.6526	0.9720	0.5537
420-440	0.0351	0.4030	0.7337
440-460	0.7058	0.3162	0.5951
460-480	0.1509	0.1328	0.7708

Table D3: p-values from the two-tailed paired t-test to study cumulation effects. Paired-pulse condition (ISI 50 ms). Trials 1-20 were compared with trials 21-40, trials 1-20 were compared with trials 41-60, and trials 21-40 were compared with trials 41-60. Avgs1==trials 1-20, avgs2==trials 21-40, avgs3==trials 41-60.

Time-window	avgs1 vs avgs2	avgs1 vs avgs3	avgs2 vs avgs3
0-20	0.3750	0.4128	0.8305
20-40	0.2230	0.4343	0.6779
40-60	0.7002	0.5211	0.3578
60-80	0.6401	0.1828	0.1393
80-100	0.3624	0.9091	0.3825
100-120	0.2870	0.2036	0.9873
120-140	0.3962	0.0415	0.0861
140-160	0.3091	0.1110	0.6473
160-180	0.7309	0.9734	0.7253
180-200	0.9639	0.4064	0.5960
200-220	0.1172	0.0030	0.0713
220-240	0.1409	0.0033	0.0868
240-260	0.2696	0.5370	0.4586
260-280	0.9992	0.9256	0.9479
280-300	0.5628	0.7649	0.7682
300-320	0.4695	0.6015	0.7725
320-340	0.2728	0.0164	0.0435
340-360	0.3798	0.0832	0.4673
360-380	0.9226	0.1466	0.1698
380-400	0.7778	0.2941	0.1674
400-420	0.9242	0.2214	0.1068
420-440	0.8529	0.0209	0.1435
440-460	0.8904	0.7467	0.9368
460-480	0.7178	0.6848	0.4132

Table D4: p-values from the two-tailed paired t-test to study cumulation effects. Paired-pulse condition (ISI 70 ms). Trials 1-20 were compared with trials 21-40, trials 1-20 were compared with trials 41-60, and trials 21-40 were compared with trials 41-60. Avgs1==trials 1-20, avgs2==trials 21-40, avgs3==trials 41-60.

Time-window	avgs1 vs avgs2	avgs1 vs avgs3	avgs2 vs avgs3
0-20	0.9823	0.7423	0.6358
20-40	0.3634	0.7874	0.3588
40-60	0.6471	0.2495	0.3017
60-80	0.6130	0.1531	0.1173
80-100	0.7740	0.4185	0.2015
100-120	0.6160	0.8530	0.6578
120-140	0.6047	0.6721	0.9833
140-160	0.0712	0.6952	0.2059
160-180	0.0917	0.4033	0.6745
180-200	0.3688	0.2272	0.9234
200-220	0.6649	0.7121	0.4284
220-240	0.6089	0.8911	0.4881
240-260	0.7785	0.8469	0.7714
260-280	0.8078	0.8926	0.5975
280-300	0.3694	0.6729	0.5065
300-320	0.8280	0.8132	0.9774
320-340	0.8537	0.7716	0.9260
340-360	0.8020	0.3699	0.5692
360-380	0.0565	0.2554	0.9640
380-400	0.0768	0.3471	0.9599
400-420	0.9030	0.2806	0.1549
420-440	0.7178	0.6191	0.3468
440-460	0.3441	0.7447	0.7196
460-480	0.5353	0.9441	0.4121

Table D5: p-values from the two-tailed paired t-test to study cumulation effects. Paired-pulse condition (ISI 90 ms). Trials 1-20 were compared with trials 21-40, trials 1-20 were compared with trials 41-60, and trials 21-40 were compared with trials 41-60. Avgs1==trials 1-20, avgs2==trials 21-40, avgs3==trials 41-60.

Time-window	avgs1 vs avgs2	avgs1 vs avgs3	avgs2 vs avgs3
0-20	0.0105	0.0214	0.2358
20-40	0.0696	0.0786	0.8110
40-60	0.1223	0.0795	0.7024
60-80	0.3396	0.3295	0.8032
80-100	0.7903	0.3159	0.4763
100-120	0.2676	0.2234	0.9608
120-140	0.4724	0.7786	0.6095
140-160	0.9505	0.7097	0.7104
160-180	0.1263	0.4494	0.3701
180-200	0.7369	0.5861	0.3756
200-220	0.6358	0.0924	0.1025
220-240	0.4440	0.1465	0.3713
240-260	0.9705	0.3562	0.1420
260-280	0.9823	0.3743	0.5305
280-300	0.9114	0.1699	0.5641
300-320	0.8069	0.3093	0.5119
320-340	0.0103	0.0633	0.6583
340-360	0.0174	0.0061	0.4836
360-380	0.0345	0.0049	0.1369
380-400	0.0030	0.0001	0.8388
400-420	0.0734	0.8495	0.0339
420-440	0.8588	0.2769	0.1624
440-460	0.7903	0.3451	0.5640
460-480	0.1267	0.0066	0.7766

Table D6: p-values from the two-tailed paired t-test to study cumulation effects. Single pulse. Trials 1-20 were compared with trials 21-40, trials 1-20 were compared with trials 41-60, and trials 21-40 were compared with trials 41-60. Avgs1==trials 1-20, avgs2==trials 21-40, avgs3==trials 41-60.

Time-window	avgs1 vs avgs2	avgs1 vs avgs3	avgs2 vs avgs3
0-20	0.5660	0.3637	0.9082
20-40	0.4648	0.2055	0.9770
40-60	0.9742	0.9947	0.9665
60-80	0.2300	0.7680	0.4005
80-100	0.0400	0.3515	0.2374
100-120	0.1288	0.1656	0.8658
120-140	0.4356	0.5627	0.9920
140-160	0.6597	0.6903	0.3944
160-180	0.3761	0.6545	0.1373
180-200	0.2368	0.4572	0.0957
200-220	0.9110	0.5815	0.4874
220-240	0.9783	0.5718	0.3794
240-260	0.4500	0.3717	0.6868
260-280	0.4331	0.1792	0.3743
280-300	0.4980	0.9848	0.4530
300-320	0.5542	0.6853	0.8296
320-340	0.2893	0.3356	0.8215
340-360	0.4861	0.2107	0.4950
360-380	0.0345	0.0049	0.1369
380-400	0.0030	0.0001	0.8388
400-420	0.0085	0.2554	0.0329
420-440	0.6979	0.1091	0.0797
440-460	0.0763	0.8997	0.1317
460-480	0.1734	0.5913	0.2061

Table D7: p-values from the two-tailed paired t-test to study cumulation effects. Single pulse on control site. Trials 1-20 were compared with trials 21-40, trials 1-20 were compared with trials 41-60, and trials 21-40 were compared with trials 41-60. Avgs1==trials 1-20, avgs2==trials 21-40, avgs3==trials 41-60.

Time-window	avgs1 vs avgs2	avgs1 vs avgs3	avgs2 vs avgs3
0-20	0.5450	0.2538	0.3582
20-40	0.6472	0.7545	0.9644
40-60	0.0286	0.6155	0.2618
60-80	0.0023	0.4182	0.0901
80-100	0.4823	0.6636	0.3345
100-120	0.1682	0.3884	0.9998
120-140	0.9602	0.9119	0.9345
140-160	0.6961	0.9795	0.7768
160-180	0.2121	0.2971	0.9771
180-200	0.6069	0.4581	0.3082
200-220	0.2193	0.6242	0.1390
220-240	0.0831	0.5233	0.4519
240-260	0.0619	0.5105	0.5593
260-280	0.9768	0.6524	0.5263
280-300	0.0293	0.8727	0.2350
300-320	0.1837	0.5291	0.4377
320-340	0.0195	0.2082	0.4458
340-360	0.7249	0.6085	0.9368
360-380	0.9864	0.4591	0.2859
380-400	0.3267	0.3262	0.0408
400-420	0.3027	0.6673	0.1883
420-440	0.0429	0.1358	0.9862
440-460	0.7402	0.1452	0.2889
460-480	0.3909	0.8685	0.2839

E Scalp maps of different paired-pulse TMS-evoked potentials

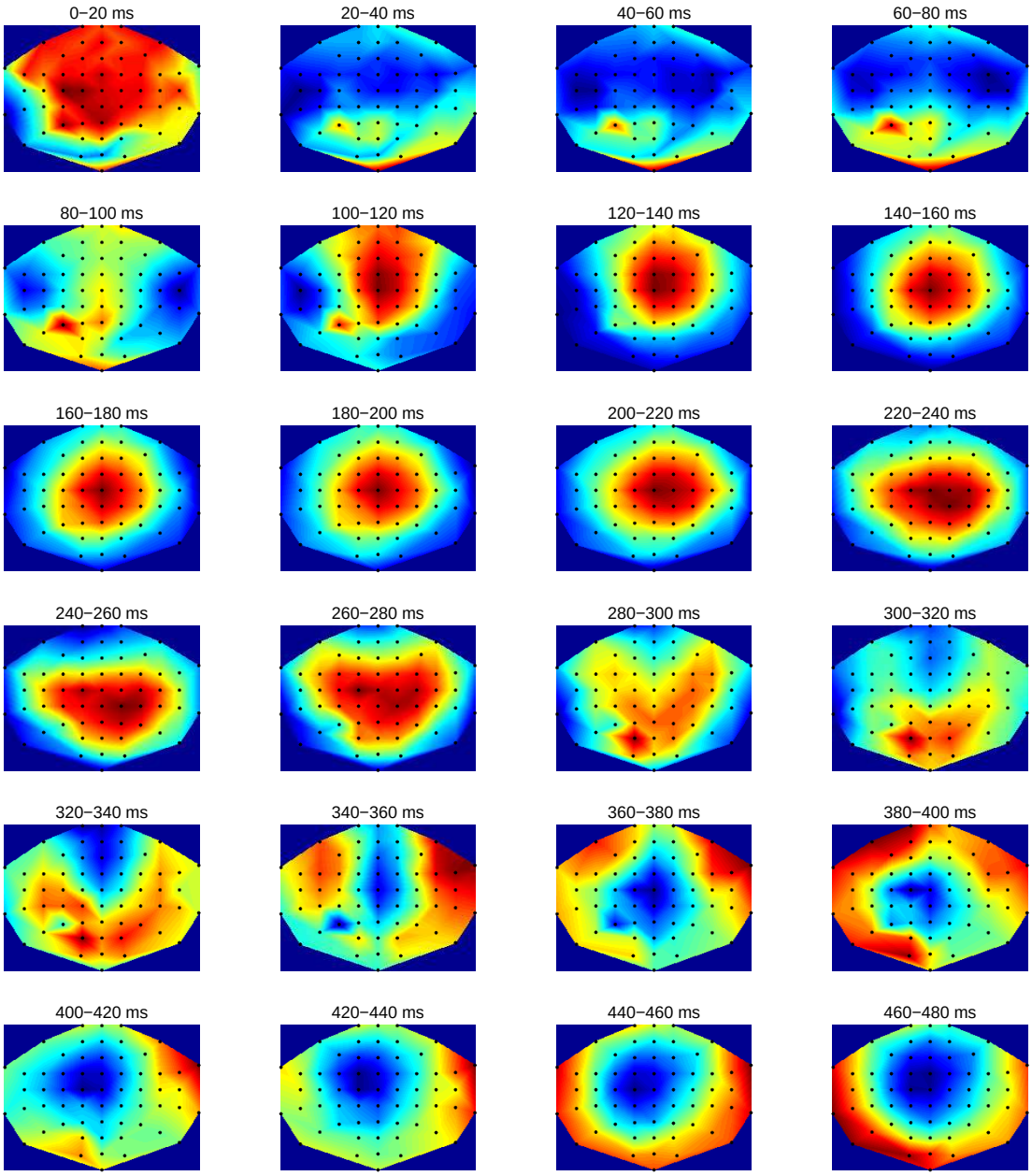

Figure E1: Scalp map of paired-pulse (ISI 30 ms) TMS-evoked EEG from primary visual cortex. The data is presented as the mean amplitude of 20 ms time windows. Zero point on time axis is the start of the second pulse. The colour red indicates positive amplitude and blue negative.

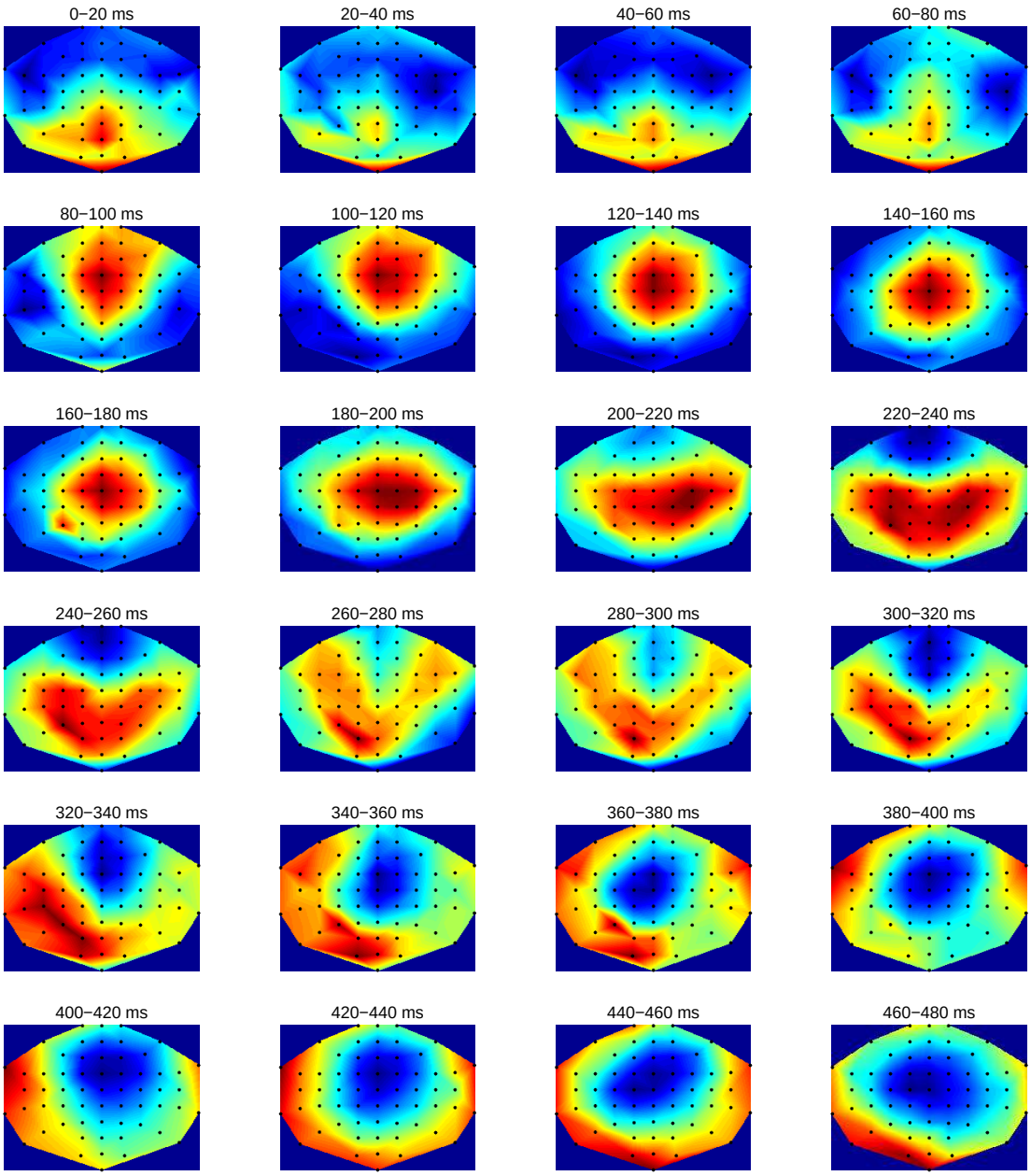

Figure E2: Scalp map of paired-pulse (ISI 50 ms) TMS-evoked EEG from primary visual cortex. The data is presented as the mean amplitude of 20 ms time windows. Zero point on time axis is the start of the second pulse. The colour red indicates positive amplitude and blue negative.

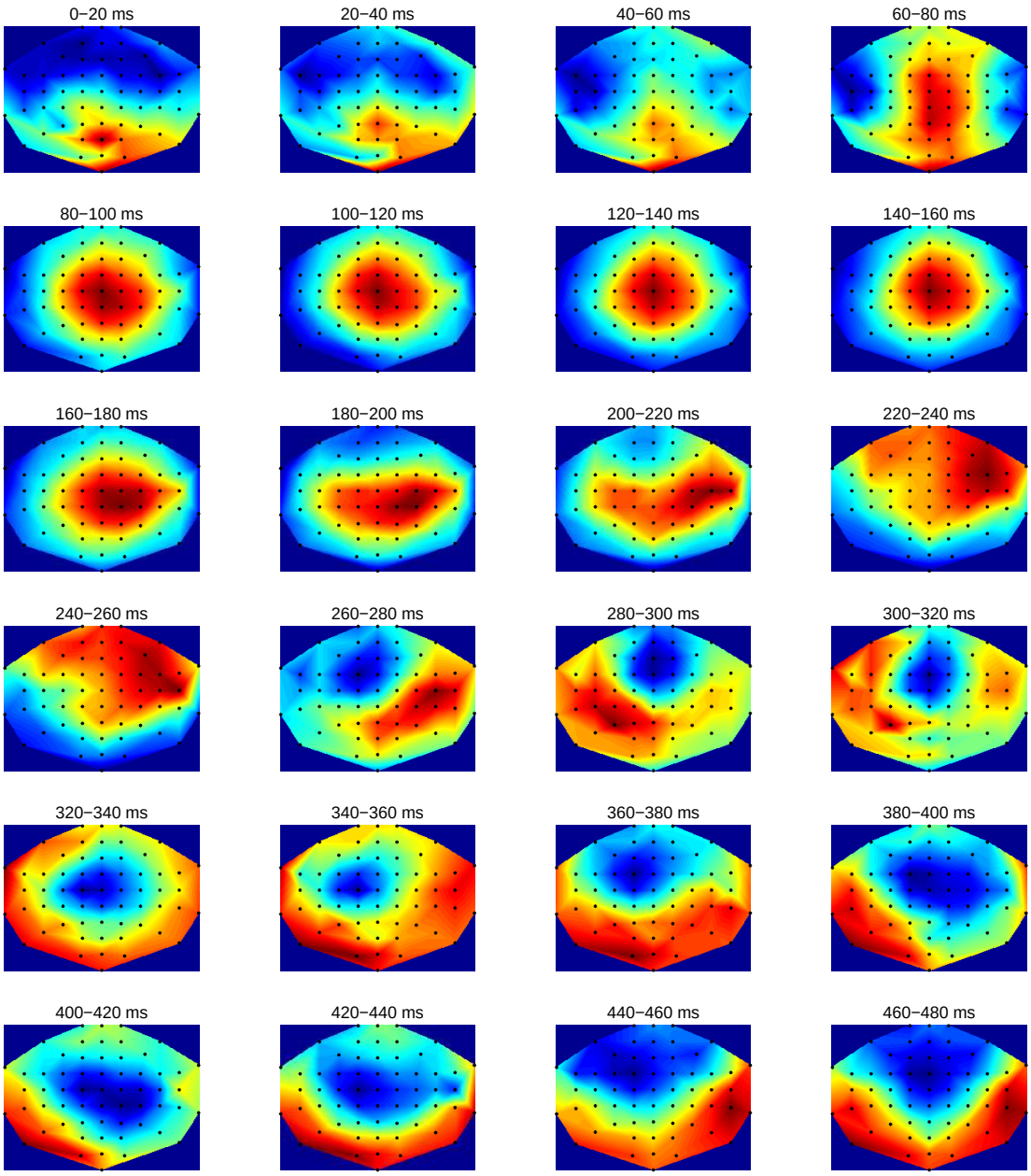

Figure E3: Scalp map of paired-pulse (ISI 70 ms) TMS-evoked EEG from primary visual cortex. The data is presented as the mean amplitude of 20 ms time windows. Zero point on time axis is the start of the second pulse. The colour red indicates positive amplitude and blue negative.

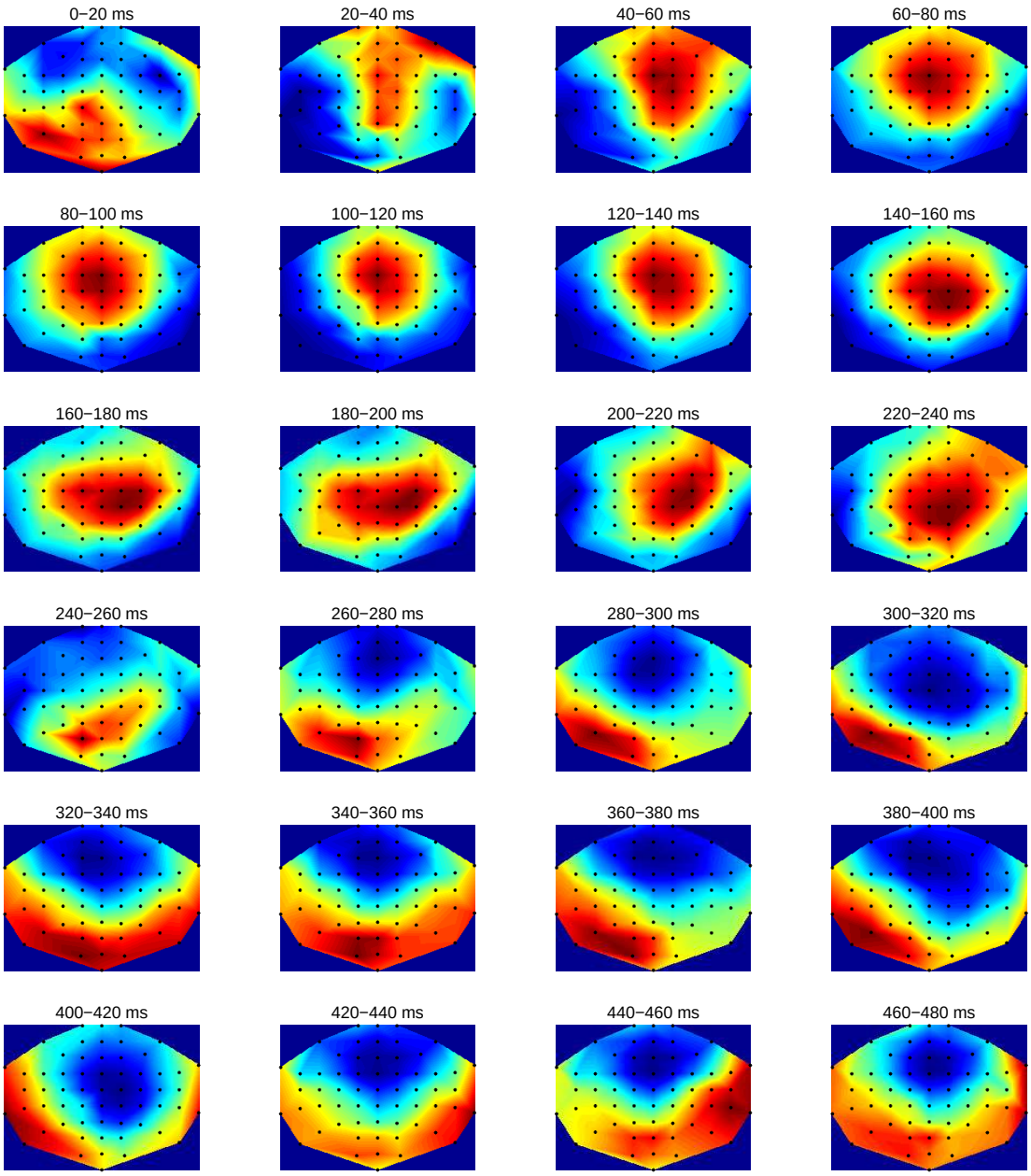

Figure E4: Scalp map of paired-pulse (ISI 90 ms) TMS-evoked EEG from primary visual cortex. The data is presented as the mean amplitude of 20 ms time windows. Zero point on time axis is the start of the second pulse. The colour red indicates positive amplitude and blue negative.

F Results from the two-tailed paired t-test from right occipital cortex, motor cortex, and dorsoprefrontal cortex.

Table F1: Results from two-tailed paired t-test on right occipital cortex. Paired-pulse protocols are compared with the single pulse protocol. Only significant results are shown.

	Paired-pulse protocols				
Time-window	10 ms	30 ms	50 ms	70 ms	90 ms
0-20 ms	p=0.030	-	-	-	-
20-40 ms	-	p=0.021	-	-	-
40-60 ms	p=0.022	-	-	-	-
60-80 ms	-	-	-	-	-
80-100 ms	-	-	-	-	-
100-120 ms	-	-	-	-	-
120-140 ms	-	-	p=0.0078	-	-
140-160 ms	-	p=0.039	-	-	-
160-180 ms	-	-	-	-	-
180-200 ms	-	-	-	-	-
200-220 ms	-	-	-	-	-
220-240 ms	-	-	-	-	-
240-260 ms	-	-	-	-	-
260-280 ms	-	-	-	-	-
280-300 ms	-	-	-	-	-
300-320 ms	-	-	-	-	-
320-340 ms	-	-	-	-	-
340-360 ms	-	-	-	-	-
360-380 ms	-	-	-	-	-
380-400 ms	-	-	-	-	-
400-420 ms	p=0.014	-	-	-	-
420-440 ms	p=0.011	-	-	-	-
440-460 ms	-	-	-	-	-
460-480 ms	-	-	-	-	-

Table F2: Results from the two-tailed paired t-test on dorsoprefrontal cortex. Paired-pulse protocols are compared with the single pulse protocol. Only significant results are shown.

	Paired-pulse protocols				
Time-window	10 ms	30 ms	50 ms	70 ms	90 ms
0-20 ms	p=0.044	-	p=0.049	p=0.020	p=0.0044
20-40 ms	-	p=0.034	p=0.0061	p=0.018	-
40-60 ms	-	-	-	-	p=0.027
60-80 ms	-	-	-	p=0.0069	p=0.00031
80-100 ms	-	p=0.0026	p=0.00072	p=1e-5	p=5e-5
100-120 ms	p=0.0068	p=7e-6	p=2e-5	p=9e-5	p=0.00035
120-140 ms	p=0.016	p=0.00045	p=0.000119	p=0.012	-
140-160 ms	-	-	-	-	-
160-180 ms	-	-	-	p=0.039	p=0.023
180-200 ms	-	p=0.040	-	p=0.00092	p=0.0039
200-220 ms	-	p=0.013	p=0.00090	-	p=0.00057
220-240 ms	-	-	-	p=0.042	p=0.00057
240-260 ms	-	-	-	-	p=0.010
260-280 ms	-	-	-	-	p=0.021
280-300 ms	-	-	-	-	p=0.022
300-320 ms	-	-	p=0.035	p=0.0041	p=0.019
320-340 ms	-	-	p=0.015	p=0.041	-
340-360 ms	-	-	-	-	-
360-380 ms	-	p=0.010	-	-	p=0.0095
380-400 ms	-	p=0.0063	-	-	p=0.0067
400-420 ms	p=0.041	-	-	-	p=0.049
420-440 ms	p=0.011	-	-	-	-
440-460 ms	-	-	-	-	-
460-480 ms	p=0.0032	-	-	-	-

Table F3: Results from the two-tailed paired t-test on the motor cortex. Paired-pulse protocols are compared with the single pulse protocol. Only significant results are shown.

	Paired-pulse protocols				
Time-window	10 ms	30 ms	50 ms	70 ms	90 ms
0-20 ms	p=0.017	-	-	-	p=0.0067
20-40 ms	-	p=0.014	p=0.013	p=0.013	p=0.033
40-60 ms	-	p=0.032	p=0.012	-	-
60-80 ms	-	p=0.016	-	-	p=0.0074
80-100 ms	-	-	p=0.011	p=0.0012	p=0.0028
100-120 ms	-	p=0.00055	p=0.00037	p=0.0023	p=0.0052
120-140 ms	-	p=0.00063	p=0.0036	-	-
140-160 ms	-	p=0.049	-	-	-
160-180 ms	-	-	-	-	p=0.028
180-200 ms	-	-	-	p=0.019	p=0.023
200-220 ms	-	-	-	-	p=0.020
220-240 ms	-	-	-	-	-
240-260 ms	-	-	-	-	p=0.0052
260-280 ms	-	-	p=0.036	-	p=0.0042
280-300 ms	-	-	-	-	p=0.0086
300-320 ms	p=0.030	-	-	-	-
320-340 ms	-	-	p=0.016	-	-
340-360 ms	-	-	p=0.043	-	-
360-380 ms	-	-	-	-	-
380-400 ms	-	p=0.0058	-	-	p=0.043
400-420 ms	p=0.018	-	-	p=0.034	p=0.0091
420-440 ms	p=0.025	-	-	p=0.017	p=0.024
440-460 ms	-	-	-	-	-
460-480 ms	p=0.027	-	-	-	-

G Frequency content of the TMS-evoked potentials

Table G1: p-values from two-tailed paired t-test to study power contents in frequency bands delta, theta, alpha, and beta.

	Frequency band			
Condition	Delta	Theta	Alpha	Beta
10 ms	0.8114	0.9704	0.5461	0.6326
30 ms	0.2001	0.4674	0.4766	0.9026
50 ms	0.7062	0.8012	0.3165	0.4323
70 ms	0.6058	0.6292	0.9361	0.4792
90 ms	0.6188	0.9074	0.4031	0.5844
control	0.2979	0.8573	0.2685	0.5308